**Table 2**
*S. venezuelensis* L3 ESTs with significant annotation by homology search against NEMABASE4.

| *S. venezuelensis* (singleton/contig) | | Top hit in Nembase4 (tblastx) | | | | |
|---|---|---|---|---|---|---|
| NCBI accession | Length (bp) | Identifier | Organism | Clade | E-value | Associated annotation |
| HO652177 | 601 | SSC02297_1 | *S. stercoralis* | IV | 4.00E−87 | Proteasome, subunit alpha/beta |
| HO652179 | 576 | CRC00223_1 | *C. remanei* | V | 5.00E−11 | RNA recognition motif, RNP-1 |
| HO652180 | 585 | SSC04545_1 | *S. stercoralis* | IV | 6.00E−45 | FMRFamide-related peptide |
| HO652192 | 348 | SSC00140_1 | *S. stercoralis* | IV | 3.00E−27 | FMRFamide-related peptide |
| HO652206 | 292 | ACC15350_1 | *A. caninum* | V | 7.00E−19 | Ammonium transporter |
| HO652209 | 759 | HBC05087_1 | *H. bacteriophora* | V | 3.00E−83 | Cytochrome b/b6 |
| HO652210 | 406 | SRC01426_1 | *S. ratti* | IV | 4.00E−51 | Cytochrome P450 |
| HO652222 | 427 | SSC01666_1 | *S. stercoralis* | IV | 1.00E−48 | Hydroxytetrahydrobiopterindehydratase |
| HO652225 | 342 | CJC00147_1 | *C. japonica* | V | 3.00E−15 | Signal recognition particle, SRP9 subunit |
| HO652234 | 761 | SRC00984_2 | *S. ratti* | IV | 1.00E−153 | Ras small GTPase, Ras type |
| HO652237 | 564 | SSC03440_1 | *S. stercoralis* | IV | 3.00E−48 | LUC7 related |
| HO652242 | 636 | MJC01056_1 | *M. javanica* | IV | 2.00E−17 | DNA repair protein (XPGC)/yeast Rad |
| HO652258 | 389 | CSC00005_1 | *Caenorhabditis sp.* | V | 1.00E−09 | NAD Hdehydrogenase (ubiquinone) |
| HO652261 | 713 | SRC00248_1 | *S. ratti* | IV | 1.00E−128 | Poly(A)-binding protein |
| HO652283 | 707 | SRC07549_1 | *S. ratti* | IV | 1.00E−108 | Calcium-binding EF-hand |
| HO652285 | 867 | XIC01943_1 | *X. index* | I | 2.00E−89 | beta-1,4-mannosyltransferase activity |
| HO652301 | 574 | SRC00826_1 | *S. ratti* | IV | 7.00E−38 | Histone H1/H5 |
| HO652303 | 620 | PTC01840_1 | *P. trichosuri* | IV | 4.00E−88 | NIF system FeS cluster assembly, NifU, N-terminal |
| HO652319 | 687 | SRC01269_1 | *S. ratti* | IV | 1.00E−111 | Neural proliferation differentiation control-1 |
| HO652339 | 828 | SSC00792_1 | *S. stercoralis* | IV | 1.00E−103 | Klarsicht/ANC-1/syne-1 homology |
| HO652341 | 817 | LSC00488_1 | *L. sigmodontis* | III | 4.00E−90 | Neurotransmitter-gated ion-channel |
| HO652363 | 569 | PTC00864_1 | *P. trichosuri* | IV | 2.00E−99 | Isocitrate lyase and phosphorylmutase |
| HO652371 | 689 | AYC01701_1 | *A. ceylanicum* | V | 1.00E−31 | HSP20-like chaperone |
| HO652385 | 324 | SRC00573_1 | *S. ratti* | IV | 2.00E−53 | Ribosome maturation protein SBDS, N-terminal |
| HO652387 | 837 | HGC09675_1 | *H. glycines* | IV | 8.00E−90 | Peptidase C2, calpain |
| HO652391 | 682 | SSC00507_1 | *S. stercoralis* | IV | 6.00E−71 | Basic helix-loop-helix dimerisation region bHLH |
| HO652393 | 304 | SRC06206_1 | *S. ratti* | IV | 1.00E−11 | Lysosome-associated membrane glycoprotein (Lamp)/CD68 |
| HO652397 | 702 | SSC03354_1 | *S. stercoralis* | IV | 4.00E−80 | Ankyrin |
| HO652402 | 806 | SRC01740_1 | *S. ratti* | IV | 1.00E−105 | TRAF-like |
| HO652403 | 702 | SSC01995_1 | *S. stercoralis* | IV | 1.00E−36 | NLI interacting factor |
| HO652411 | 638 | AAC00359_1 | *A. cantonensis* | V | 4.00E−39 | Neurotransmitter-gated ion-channel |
| HO652429 | 713 | SRC03434_1 | *S. ratti* | IV | 1.00E−96 | Alpha/beta hydrolase fold-1 |
| HO652446 | 591 | PTC02320_1 | *P. trichosuri* | IV | 6.00E−45 | Zinc finger, C3HC4 RING-type |
| HO652452 | 642 | ACC01684_2 | *A. caninum* | V | 7.00E−42 | Globin-like |
| HO652470 | 681 | PTC01361_1 | *P. trichosuri* | IV | 2.00E−23 | Bicarbonate transporter, eukaryotic |
| HO652471 | 586 | SRC00877_1 | *S. ratti* | IV | 2.00E−99 | NADH:ubiquinone oxidoreductase, 51 kDa subunit |
| HO652478 | 385 | SSC01554_1 | *S. stercoralis* | IV | 2.00E−41 | Neuroendocrine 7B2 precursor |
| HO652504 | 687 | CRC01991_1 | *C. remanei* | V | 1.00E−47 | Oxysterol-binding protein |
| HO652510 | 481 | SSC05747_1 | *S. stercoralis* | IV | 1.00E−44 | Barrier to autointegration factor, BAF |
| HO652512 | 799 | SRC00306_1 | *S. ratti* | IV | 1.00E−152 | 14-3-3 protein |
| HO652514 | 263 | SRC02616_1 | *S. ratti* | IV | 2.00E−50 | C2 calcium-dependent membrane targeting |
| HO652517 | 526 | SSC02701_1 | *S. stercoralis* | IV | 1.00E−75 | Histone H2B |
| HO652520 | 545 | CBC03783_1 | *C. brenneri* | V | 2.00E−41 | Glycosyl transferase, group 1 |
| HO652521 | 479 | CSC01296_1 | *Caenorhabditis sp.* | V | 1.00E−21 | RhoGAP |
| HO652553 | 286 | SSC00283_1 | *S. stercoralis* | IV | 4.00E−29 | Heat-shock protein Hsp90 |
| HO652559 | 336 | SSC02701_1 | *S. stercoralis* | IV | 5.00E−36 | Histone H2B |
| HO652574 | 361 | SRC08538_1 | *S. ratti* | IV | 9.00E−31 | L3Nie Ag (SvL3Nie-2) |
| HO652576 | 666 | SSC00003_1 | *S. stercoralis* | IV | 1.00E−86 | Astacin-like metalloproteinase |
| HO652580 | 406 | MHC11486_1 | *M. hapla* | IV | 1.00E−07 | Amino acid/polyamine transporter I |
| HP429054 | 589 | HBC06265_1 | *H. bacteriophora* | V | 3.00E−47 | Globin-like protein |
| HP429057 | 461 | SSC01535_1 | *S. stercoralis* | IV | 3.00E−19 | S. stercoralis Hsp20 (SvHsp20-Ss2) |
| HP429059 | 565 | ASC17349_1 | *A. suum* | III | 2.00E−23 | A. suum Hsp20 (SvHsp20-As1) |
| HP429060 | 508 | SSC00303_1 | *S. stercoralis* | IV | 2.00E−15 | Lipase, class 2 |
| HP429061 | 455 | SSC00007_1 | *S. stercoralis* | IV | 7.00E−68 | Aminotransferase, class I and II |
| HP429062 | 1558 | OOC00027_4 | *O. ostertagi* | V | 0 | Cytochrome c oxidase, subunit I |
| HP429068 | 655 | SRC08538_1 | *S. ratti* | IV | 7.00E−70 | L3Nie Ag (SvL3Nie-1) |
| HP429076 | 762 | SSC02252_1 | *S. stercoralis* | IV | 1.00E−122 | EF-hand |
| HP429077 | 441 | SRC00553_1 | *S. ratti* | IV | 1.00E−35 | Calcium-binding EF-hand |
| HP429078 | 524 | TLC00048_1 | *T. leonina* | III | 3.00E−62 | Cytochrome c oxidase, subunit III |
| HP429079 | 628 | SRC00445_1 | *S. ratti* | IV | 6.00E−97 | EF-hand |
| HP429083 | 889 | SSC00456_1 | *S. stercoralis* | IV | 1.00E−70 | Proteinase inhibitor I33, aspin |
| HP429085 | 863 | CJC01127_2 | *C. japonica* | V | 5.00E−45 | NADH:ubiquinone/plastoquinone oxidoreductase |
| HP429086 | 480 | ASC00025_17 | *A. suum* | III | 4.00E−76 | Cytochrome c oxidase subunit II C-terminal |
| HP429088 | 417 | SRC04160_1 | *S. ratti* | IV | 4.00E−42 | Light chain 3 (LC3) |
| HP429091 | 661 | SSC01535_1 | *S. stercoralis* | IV | 4.00E−78 | S. stercoralis Hsp20 (SvHsp20-Ss1) |
| HP429092 | 1322 | SSC05809_1 | *S. stercoralis* | IV | 2.00E−62 | Methyltransferase type 11 |
| HP429094 | 277 | NAC00065_1 | *N. americanus* | V | 3.00E−16 | Cytochrome b/b6, C-terminal |
| HP429095 | 589 | ASC24228_1 | *A. suum* | III | 2.00E−19 | ATPase, F0 complex, subunit A |

Genus designations used in the table are as follows: *A. caninum*; *Ancylostoma caninum*, *A. cantonensis*; *Angiostrongylus cantonensis*, *A. ceylanicum*; *Ancylostoma ceylanicum*, *A. suum*; *Acaris suum*, *C. brenneri*; *Caenorhabditis brenneri*, *C. japonica*; *Caenorhabditis japonica*, *C. remanei*; *Caenorhabditis remanei*, *H. bacteriophora*; *Heterorhabditis bacteriophora*, *H. glycines*; *Heterodera glycines*, *L. sigmodontis*; *Litomosoides sigmodontis*, *M. hapla*; *Meloidogyne hapla*, *M. javanica*; *Meloidogyne javanica*, *N. americanus*; *Necator americanus*, *O. ostertagi*; *Ostertagia ostertagi*, *P. trichosuri*; *Parastrongyloides trichosuri*, *S. ratti*; *Strongyloides ratti*, *S. stercoralis*; *Strongyloides stercoralis*, *T. leonina*; *Toxascaris leonina*, *X. index*; *Xiphinema index*.

**Table 3**
*S. venezuelensis* L3 ESTs with significant annotation against NCBI non-redundant protein database.

| *S. venezuelensis* (singleton/contig) | | Top hit in the NCBI non-redundant protein database (blastx) | | | | Top hit in Nembase4 (tblastx) | | | |
|---|---|---|---|---|---|---|---|---|---|
| NCBI accession | Length (bp) | NCBI accession | Best identity descriptor | Organism | E-value | Identifier | Organism | Clade | E-value |
| HO652462 | 820 | NP_501872.1 | hypothetical protein F01G10.6 | *C. elegans* | 3.00E−12 | N/F[a] | – | – | – |
| HO652207 | 396 | XP_002636737.1 | Hypothetical protein CBG23460 | *C. briggsae* | 4.00E−15 | PTC02337_1 | *P. trichosuri* | IV | 2.00E−21 |
| HO652218 | 448 | XP_002633793.1 | Hypothetical protein CBG03485 | *C. briggsae* | 6.00E−22 | HCC05184_1 | *H. contortus* | V | 4.00E−33 |
| HO652251 | 849 | XP_002632491.1 | CBR-CCG-1 protein | *C. briggsae* | 2.00E−49 | SRC00347_1 | *S. ratti* | IV | 1.00E−140 |
| HO652337 | 409 | XP_001892281.1 | hypothetical protein | *B. malayi* | 6.00E−38 | PPC05674_1 | *P. pacificus*[b] | V | 8.00E−50 |
| HO652351 | 463 | XP_002631908.1 | hypothetical protein CBG07885 | *C. briggsae* | 2.00E−37 | PTC00166_1 | *P. trichosuri* | IV | 5.00E−53 |
| HO652377 | 395 | XP_001902589.1 | putative salt tolerance protein | *B. malayi* | 5.00E−19 | PTC04384_1 | *P. trichosuri* | IV | 4.00E−61 |
| HO652412 | 835 | XP_002645282.1 | CBR-AJM-1 protein | *C. briggsae* | 3.00E−09 | SSC03769_1 | *S. stercoralis* | IV | 8.00E−65 |
| HO652449 | 581 | NP_499054.1 | TransThyretin-Related family domain family member (ttr-5) | *C. elegans* | 9.00E−33 | SRC01281_1 | *S. ratti* | IV | 2.00E−84 |
| HO652459 | 286 | NP_510509.2 | hypothetical protein F09B12.3 | *C. elegans* | 1.00E−14 | SRC04118_1 | *S. ratti* | IV | 2.00E−34 |
| HO652491 | 650 | XP_001902568.1 | hypothetical protein Bm1_55555 | *B. malayi* | 1.00E−27 | SSC01022_1 | *S. stercoralis* | IV | 2.00E−85 |
| HO652499 | 797 | NP_505173.2 | hypothetical protein F52E1.13 | *C. elegans* | 3.00E−43 | CRC02974_1 | *C. remanei* | V | 5.00E−20 |
| HO652537 | 528 | NP_499054.1 | TransThyretin-Related family domain family member (ttr-5) | *C. elegans* | 2.00E−30 | SRC01281_1 | *S. ratti* | IV | 4.00E−78 |
| HO652548 | 533 | XP_002646626.1 | Hypothetical protein CBG11056 | *C. briggsae* | 8.00E−10 | SRC02345_1 | *S. ratti* | IV | 3.00E−57 |
| HP429066 | 2081 | NP_492698.2 | hypothetical protein ZC247.1 | *C. elegans* | 1.00E−71 | SSC03002_1 | *S. stercoralis* | IV | 6.00E−72 |
| HP429084 | 856 | CAR63582.1 | Conserved Cystein/Glycine domain protein | *A. cantonensis* | 1.00E−41 | SRC00347_1 | *S. ratti* | IV | 1.00E−129 |

*S. venezuelensis* L3i ESTs that did not hit in NEMABASE4 or ESTs which had matches to NEMABASE4 ESTs without annotation, were further analysed against NCBI non-redundant protein database. Sixteen EST were given annotation by this search.
[a] N/F: no hit in NEMABASE4.
[b] *Pristionchus pacificus*.

comprised the unique sequences, which were compared against NEMBASE4 (http://www.nematodes.org/ nembase4/), using tBLASTx. ESTs that did not hit were further compared with the National Center for Biotechnology Information (NCBI) non-redundant protein database using BLASTx (cut-off: E<1e−5), and NCBI EST database using BLASTn (cut-off: E<1e−10). The sequences of the transcripts in the

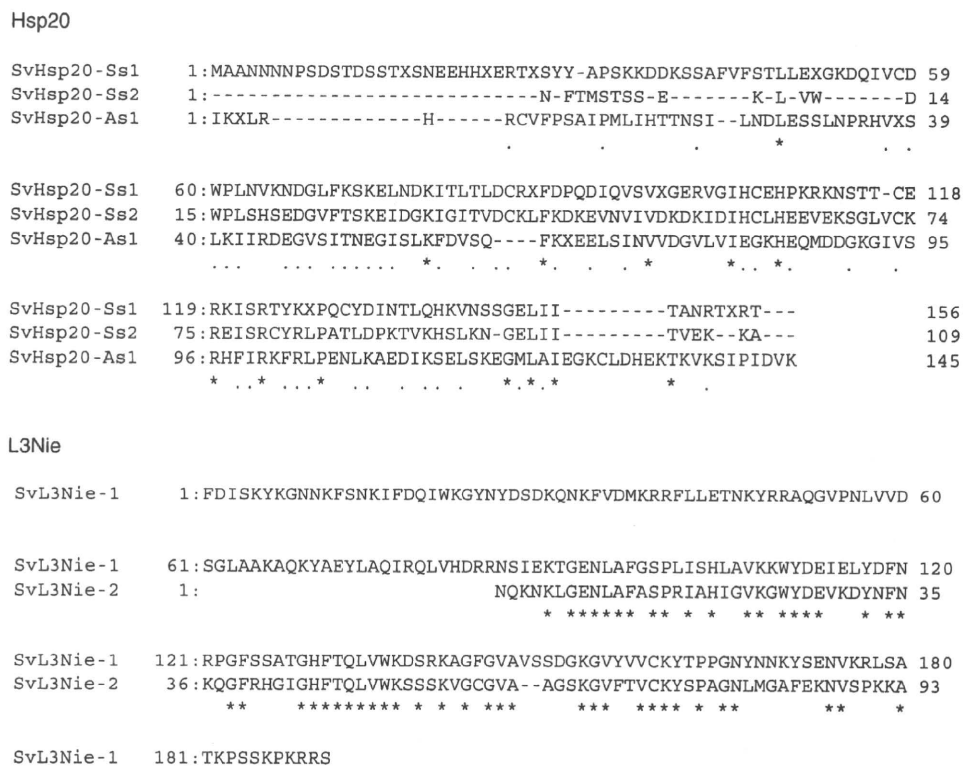


**Fig. 1.** Comparison of predicted amino acid sequences between three Hsp20s and two L3Nie antigens. In *S. venezuelensis* ESTs, three different Hsp20 and two L3Nie were found. In order to clarify the difference between these ESTs, they were aligned against each other by using the GENETYX-WIN software (GENETYX CORPORATION, Tokyo, Japan). Identical residues are marked with an asterisk, and conserved residues between two Hsp20s are marked with a dot. SvHsp20-Ss1 showed 40% identity to SvHsp20-Ss2. SvHsp20-As1 was found to have 29% identity with SvHsp20-Ss2, but no significant similarity with SvHsp20-Ss1. Identity between SvL3Nie-1 and 2 was 56%. Accession numbers for each genes: SvHSP20-Ss1; HP429091, SvHSP20-Ss2; HP429057, SvHSP20-As1; HP429059, SvL3Nie-1; HP429068, SvL3Nie-2; HO652574.

present study have been deposited into the GenBank under accession numbers HO652177–HO652584 and HP429054–HP429095.

### 2.5. Reverse transcriptase-polymerase chain reaction (RT-PCR)

RT-PCR was performed with worms of different developmental stages; infective larvae (L3i), tissue-migrating larvae (L3tm), lung larvae (LL3), and parasitic adult worms. For RNA isolation, worms were crushed manually using a freeze-crushing apparatus (SK Mill, Tokken, Chiba, Japan), followed by isolation with TRIzol reagent. After treatment with DNase I (Ambion, Austin, TX, USA), concentration of RNA was measured using a Quant-iT assay kit (Invitrogen). cDNA was synthesized from 1 μg of total RNA by reverse transcription in 100 μl reaction using PrimeScript 1st strand cDNA Synthesis Kit (Takara Bio, Shiga, Japan).

For 63 selected genes, PCR primers were designed to have theoretical Tm of 57–63 °C and amplicon sizes of 200–500 bp. One microliter of the prepared cDNA preparation was used for PCR amplification. The amplification program was as follows; initial denaturation at 94 °C for 2 min, 30 cycles of denaturation at 94 °C for 45 s, annealing 58 °C for 45 s and elongation at 68 °C for 30 s, followed by a final extension at 68 °C for 7 min. Five microliter of the PCR products was mixed with 1 μl of EZ-VISION DNA dye/buffer (AMRESCO, Solon, OH, USA ), run on 1% agarose gel, then visualized by UV transillumination and photographed.

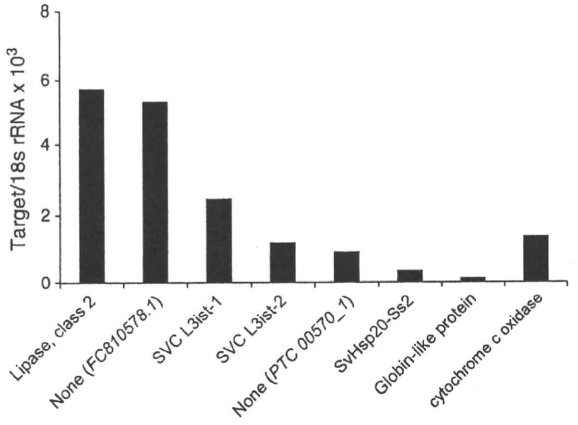


**Fig. 2.** Expression analysis of abundant transcripts in infective larvae. Quantification of transcripts was achieved by real-time PCR using gene-specific primer sets for the top 8 sequences (Table 4). The gene for a class 2 lipase was the most abundantly transcribed in L3i, which was followed by novel genes of unknown functions. The target values were normalized to 18S rRNA expression. Accession numbers for each genes: lipase; HP429060, *FC810578.1*; HP429073, SVC L3ist-1; HP429055, SVC L3ist-2; , HP429056, *PTC 00570_1*; HP429058, SvHsp20-Ss2; HP429057, Globin-like protein; HP429054, cytochrome *c* oxidase; HP429062.

### 2.6. Real-time PCR analyses

Expression of selected transcripts was analyzed in real-time PCR. The regions amplified with each primer sets were shown in Table 1. Total RNA was extracted from different stages of larvae as described above, and cDNA was generated from 400 ng of RNA using Prime-Script 1st strand cDNA Synthesis Kit (Takara Bio). Real-time PCR was then performed with an ABI PRISM 7000 Sequence Detection Systems and a Power SYBR Green PCR Master Mix (Applied Biosystems). Relative quantification was assessed by normalizing the amount of the target transcript to 18S ribosomal RNA gene.

## 3. Results

A cDNA library was constructed from infective larvae of *S. venezuelensis*. A total of 500 clones were sequenced producing 408 high quality ESTs (250 bp cut-off) with an average of 490 ± 164 bp. Assembling the 408 ESTs resulted in 42 contigs (288 ESTs) and 120

**Table 4**
The most abundant transcripts in *S. venezuelensis* L3i cDNA library.

| *S. venezuelensis* (singleton/contig) | | Blast top hit against NEMABASE4 | | | |
|---|---|---|---|---|---|
| NCBI accession | Number of clones | Identifier | Organism | E-value | Associated annotation |
| HP429060 | 38 | SSC00303_1 | *S. stercoralis* | 2.00E−15 | Lipase, class 2 |
| HP429056 | 33 | Novel[a] (SVC L3ist-2) | – | – | – |
| HP429054 | 29 | HBC06265_1 | *H. bacteriophora* | 3.00E−47 | Globin-like protein |
| HP429055 | 27 | Novel[a] (SVC L3ist-1) | – | – | – |
| HP429057 | 26 | SSC01535_1 | *S. stercoralis* | 3.00E−19 | S. stercoralis Hsp20 (SvHsp20-Ss2) |
| HP429073 | 14 | FC810578.1[b] | *S. ratti* | 5.00E−13 | None |
| HP429058 | 10 | PTC00570_1 | *P. trichosuri* | 3.00E−29 | None |
| HP429062 | 8 | OOC00027_4 | *O. ostertagi* | 0 | Cytochrome *c* oxidase, subunit I |
| HP429064 | 7 | Novel[a] | – | – | – |
| HP429079 | 6 | SRC00445_1 | *S. ratti* | 6.00E−97 | EF-hand |
| HP429066 | 5 | SSC03002_1 | *S. stercoralis* | 6.00E−72 | None |
| HP429070 | 5 | SRC01349_1 | *S. ratti* | 2.00E−19 | None |
| HP429075 | 5 | SSC00031_1 | *S. stercoralis* | 5.00E−70 | None |
| HP429076 | 4 | SSC02252_1 | *S. stercoralis* | 1.00E−122 | EF-hand |
| HP429085 | 4 | CJC01127_2 | *C. japonica* | 5.00E−45 | NADH:ubiquinone/plastoquinone oxidoreductase |
| HP429072 | 4 | SRC01349_1 | *S. ratti* | 2.00E−22 | None |
| HP429067 | 4 | Novel[a] | – | – | – |
| HP429069 | 4 | Novel[a] | – | – | – |
| HP429059 | 3 | ASC17349_1 | *A. suum* | 2.00E−23 | A. suum Hsp20 (SvHsp20-As1) |
| HP429068 | 3 | SRC08538_1 | *S. ratti* | 7.00E−70 | L3Nie Ag (SvL3Nie-1) |
| HP429084 | 3 | SRC00347_1 | *S. ratti* | 1.00E−129 | None |
| HP429081 | 3 | SRC07826_1 | *S. ratti* | 4.00E−37 | None |
| HP429074 | 3 | SSC04537_1 | *S. stercoralis* | 2.00E−07 | None |
| HP429087 | 3 | Novel[a] | – | – | – |
| HP429065 | 3 | Novel[a] | – | – | – |

[a] Novel; No hits were found in major public databases.
[b] All hits shown here were found against Nembase4 except for FC810578.1, which was found a match in NCBI EST database only.

singletons. tBLASTx analysis against NEMABASE4, a comprehensive resource for nematode transcriptome analysis holding 679,480 nematode EST, resulted in 114 (70.4%) *S. venezuelensis* L3i ESTs showing significant (E<1e−5) matches to nematode EST, in which associated annotation was given to 68 sequences (Table 2).

*S. venezuelensis* L3i ESTs that did not hit in NEMABASE4 and the ones which had matches to NEMABASE4 ESTs without annotation, were further analyzed by BLASTx against the NCBI non-redundant protein databases. This search yielded 16 more genes with description (Table 3). Thus in total, 84 ESTs resulted in significant annotation against the major public databases. It should be noted that most of the hits in NEMABASE4 were genes of clade IV nematode, and a majority of the clade IV hits were with genes from *Strongyloides* (Tables 2 and 3).

Some *S. venezuelensis* L3i ESTs shown in Table 2 hit the same sequences in databases. For example, HP429091 and HP429057 hit *S. stercoralis* Hsp20 (SSC01535_1), and HP429068 and HO652574 hit *S. ratti* L3Nie Ag (SRC08538_1). Sequence alignment of these ESTs revealed that they differed significantly from each other (Fig. 1). Therefore, they were considered as different gene products and designated as shown in Fig. 1.

Of 162 *S. venezuelensis* L3i ESTs, 47 gave no hits in NCBI databases or NEMABASE4 in BLASTx and tBLASTx, respectively. We compared these sequences with NCBI EST division in BLASTn to find 7 more hits (E<1e−10). Thus of 162 unique sequences, 37 (22.3%) had no hits against NCBI or NEMABASE4, indicating that these were novel genes.

Matched transcripts with significant annotation (84 sequences) could be grouped into some categories: genes for proteins involved in oxidative phosphorylation, structural proteins, heat-shock proteins, neuromuscular proteins, and immunodominant proteins. Interesting transcripts were also found such as calpain (HO652387, Table 2), astacin-like metalloproteinase (HO652576, Table 2), salt tolerance protein (HO652377, Table 3), DNA repair protein (HO652242, Table 2), and autophagy-related LC3 (HP429088, Table 2).

The most abundant transcripts in *S. venezuelensis* infective larva, estimated from the frequency of clones, contained class 2 lipase, globin-like protein, and small heat-shock protein 20, SvHsp20-Ss2, similar to *S. stercoralis* Hsp20. However, a number of abundant transcripts had no hits even against NCBI EST using BLASTn (Table 4), suggesting that infective larvae probably express a number of species-specific genes. In order to examine the relative amount of expression of these seemingly abundant transcripts in L3i, we performed real-time PCR for the top 8 sequences containing 4 unannotated ESTs. We found that the gene for a class 2 lipase was the most abundantly transcribed in L3i, which was followed by novel genes and genes of unknown functions (Fig. 2). Two genes, *S. venezuelensis* L3i-specific transcript 1 and 2 (SVC L3ist-1 and SVC L3ist-2), had no hits in nucleotide databases by BLASTn analysis, indicating that these were novel genes.

Because infective larvae have to survive stressful environment, we examined in real-time PCR the gene expression of heat-shock proteins and energy-related proteins in different developmental stages. Expression profile of the heat-shock proteins differed from each other. As shown in Table 2, we obtained one Hsp90 and three Hsp20

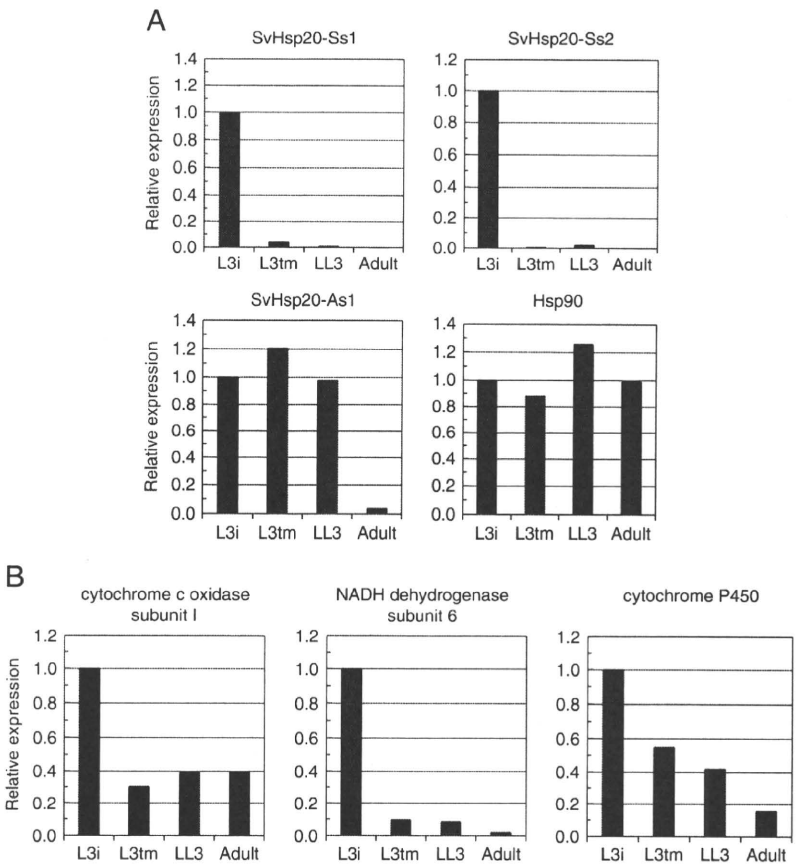


**Fig. 3.** Comparison of mRNA expression in developmental stages. Real-time PCR was performed with infective larvae (L3i), tissue-migrating larvae (L3tm), lung larvae (LL3) and adult female worms. (A) Expression profile of the heat-shock proteins. Hsp90 was evenly expressed through all developmental stages, while the expression of SvHsp20-As1 was decreased in adult worm. SvHsp20-Ss1 was expressed only in the infective larva stage differed from each other. (B) Gene expression of energy-related proteins. Genes, including cytochrome *c* oxidase subunit I, NADH dehydrogenase subunit 6, and cytochrome P450, were most actively transcribed in the infective larva stage. Relative expression of the target genes was assessed by normalizing to 18S rRNA expression. Gene expression in L3i was defined as 1.0. Accession numbers for each genes: SvHsp20-Ss1; HP429091, SvHsp20-Ss2; HP429057, SvHsp20-As1; HP429059, Hsp90; HO652553, cytochrome *c* oxidase; HP429062, NADH dehydrogenase; HO652258, cytochrome P450; HO652210.

sequences. Since these three Hsp20 (HP429091, HP429057, and HP429059) differed significantly from each other (Fig. 1), they were referred to as SvHsp20-Ss1, SvHsp20-Ss2, and SvHsp20-As1, respectively. While Hsp90 was expressed evenly from infective larvae to parasitic adult females, the expression of SvHsp20-As1 decreased when the worms reached maturity. In contrast, SvHsp20-Ss1 and SvHsp20-Ss2 were expressed only in the infective larva stage (Fig. 3A).

Genes for spiration-related proteins, including cytochrome *c* oxidase subunit I (HP429062), NADH dehydrogenase (HO652258), and cytochrome P450 (HO652210), were most actively transcribed in the infective larva stage (Fig. 3B), suggesting that infective larvae are active in producing ATP by oxidative phosphorylation. In fact, infective larvae had batteries of well-developed mitochondria immediately under the muscular layer demonstrated by transmission electron microscopy (data not shown).

In order to identify L3i-specific transcripts, which could be the clues to the elucidation of the survival strategy of infective larvae, we compared the expression pattern along the developmental stages of 62 genes by RT-PCR, containing 57 annotated and 5 non-annotated but highly abundant genes listed in Table 4. cDNA was prepared from infective larvae (L3i), tissue-migrating larvae (L3tm), lung larvae (LL3), and parasitic adult female worms, was amplified in PCR followed by the examination on agarose gel. PCR products were successfully obtained for 52 transcripts, revealing 7 transcripts being specific for infective larva stage (Table 5).

To confirm the stage specificity of these genes, we examined the expression in real-time PCR. Among 7 L3i specific transcripts listed in Table 5, the specific expression of SvHsp20-Ss1 and SvHsp20-Ss2, has been already demonstrated in Fig. 3. As shown in Fig. 4, the expression of the remaining 5 genes was highly specific as well for infective larvae. In addition to SvHsp20-Ss1 and SvHsp20-Ss2, L3i-specific transcripts were astacin-like metalloprotease, SvL3Nie-2, an unannotated gene (*PTC 00570_1*), and two novel transcripts (SVC L3ist-1 and SVC L3ist-2). Quite interestingly, SvL3Nie-1, which is similar to SvL3Nie-2, showed different expression patterns with SvL3Nie-2. SvL3Nie-1 was expressed constitutively from L3i to tissue-migrating L3tm stage (Fig. 4).

**Table 5**
Expression of transcripts along developmental stages.

| *S. venezuelensis* (singleton/contig) | | Best identity descriptor |
|---|---|---|
| Expression | NCBI accession | |
| L3i only | HO652574 | SvL3Nie-2 |
| | HO652576 | Astacin-like metalloproteinase |
| | HP429055 | Novel[a] (SVC L3ist-1) |
| | HP429056 | Novel[a] (SVC L3ist-2) |
| | HP429057 | SvHsp20-Ss2 |
| | HP429058 | None (PTC 00570_1)[b] |
| | HP429091 | SvHsp20-Ss1 |
| L3i to L3tm | HP429068 | SvL3Nie-1 |
| L3i to LL3 | HO652180 | FMRFamide-related peptide |
| | HO652403 | NLI interacting factor |
| | HO652411 | Neurotransmitter-gated ion-channel |
| | HP429054 | Globin-like protein |
| | HP429059 | SvHsp20-As1 |
| | HP429061 | Aminotransferase, class I and II |
| | HP429076 | EF-hand |
| | HP429077 | Calcium-binding EF-hand |
| | HP429088 | Light chain 3 (LC3) |
| L3i to adult | HO652177 | Proteasome, subunit alpha/beta |
| | HO652206 | Ammonium transporter |
| | HO652234 | Ras small GTPase, Ras type |
| | HO652242 | DNA repair protein (XPGC)/yeast Rad |
| | HO652251 | C. briggsae CBR-CCG-1 protein[c] |
| | HO652258 | NADH dehydrogenase subunit 6 |
| | HO652261 | Poly(A)-binding protein |
| | HO652285 | beta-1,4-mannosyltransferase activity |
| | HO652301 | Histone H1/H5 |
| | HO652303 | NIF system FeS cluster assembly, NifU, N-terminal |
| | HO652319 | Neural proliferation differentiation control-1 |
| | HO652339 | Klarsicht/ANC-1/syne-1 homology |
| | HO652341 | Neurotransmitter-gated ion-channel |
| | HO652363 | Isocitrate lyase and phosphorylmutase |
| | HO652371 | HSP20-like chaperone |
| | HO652385 | Ribosome maturation protein SBDS, N-terminal |
| | HO652387 | Peptidase C2, calpain |
| | HO652397 | Ankyrin |
| | HO652412 | *C. briggsae* CBR-AJM-1 protein[c] |
| | HO652449 | TransThyretin-Related family domain family member[c] |
| | HO652459 | hypothetical protein F09B12.3[c] |
| | HO652470 | Bicarbonate transporter, eukaryotic |
| | HO652504 | Oxysterol-binding protein |
| | HO652510 | Barrier to autointegration factor, BAF |
| | HO652514 | C2 calcium-dependent membrane targeting |
| | HO652517 | Histone H2B |
| | HO652520 | Glycosyl transferase, group 1 |
| | HO652537 | TransThyretin-Related family domain family member[c] |
| | HO652553 | Heat-shock protein Hsp90 |
| | HP429060 | Lipase, class 2 |
| | HP429062 | Cytochrome c oxidase, subunit I |
| | HP429073 | None[b] |
| | HP429083 | Proteinase inhibitor I33, aspin |
| | HP429084 | Putative conserved cystein/glycine domain protein[c] |
| | HP429092 | Methyltransferase type 11 |

[a] Novel; No hits were found in major databases.
[b] Hits were found in NEMABASE4 with no associated annotation.
[c] Hits were found in NEMABASE4 without associated annotation. Annotation was given in NCBI NR protein database.

## 4. Discussion

Most cases of strongyloidiasis are subclinical, and chronic infections remain unrecognized for decades [14]. However, it might turn life-threatening when the patients are on immunosuppressive drugs [15] or have co-infections with HTLV-1 [16–18]. In severe strongyloidiasis, large numbers of infective larvae penetrate skin and intestinal mucosa causing disseminated infections. Understanding the biology of infective larvae would lead us to find a novel strategy for the control of severe infections.

Our present study on transcripts of *S. venezuelensis* infective larva revealed interesting features of their biology. First, in the present cDNA library, clones coding for lipase appeared repeatedly. Representation in a cDNA library generally reflects the abundance in the original transcriptome [19], and the real-time PCR results confirmed lipase as one of the most actively transcribed genes (Fig. 2). It appears that infective larvae of *S. venezuelensis* possibly degrade stored lipid for energy generation. Because infective larvae do not feed during wait [20], and express both an autophagosome marker LC3 (HP429088 in Table 2) and a proteasome protein (HO652177 in Table 2), infective larvae possibly depend on both the ubiquitin–proteasome system and autophagy processes for the energy sources. Recent study has revealed that autophagy regulates intracellular lipid metabolism [21], which is evoked when animals are under starvation [22–24].

Transcripts for several different heat-shock proteins were found in *S. venezuelensis* infective larvae cDNA. Hsp90, an evolutionarily conserved indispensable molecular chaperone, is involved in the folding, stabilization, activation, and assembly of a wide range of cellular proteins, playing a central role in many biological processes [25]. In *C. elegans*, Hsp90 is upregulated in dauer larvae, to which infective larvae of parasitic nematodes are often compared [26]. Our present study demonstrated that Hsp90 is abundantly and constitutively transcribed throughout the life of *S. venezuelensis* (Fig. 3A). In spite of a number of similarities between infective larvae and dauer larvae, recent comparative genomics between *C. elegans* and

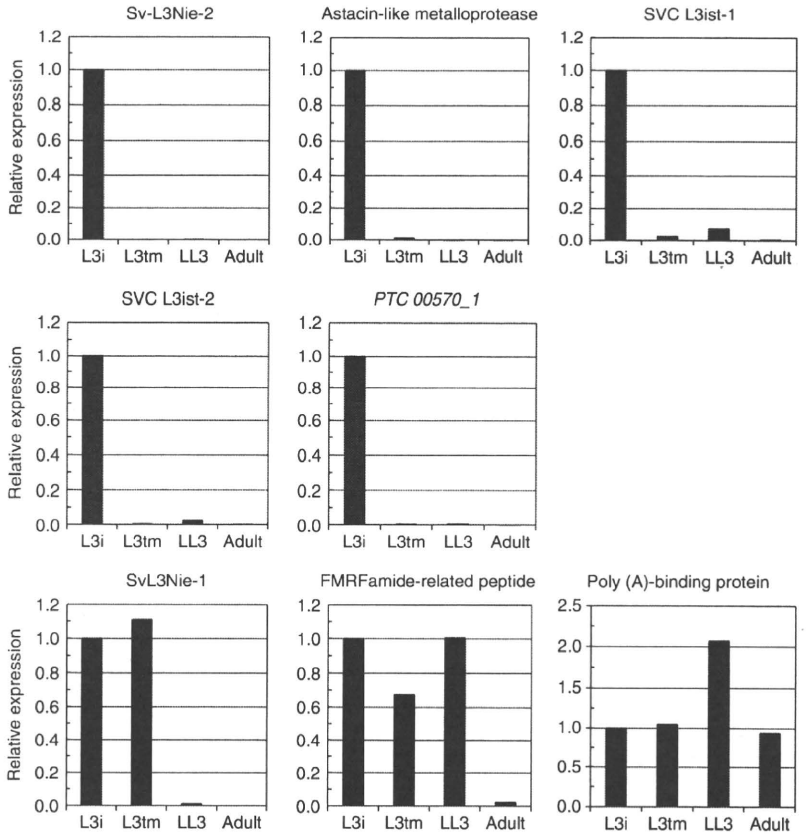


**Fig. 4.** Quantitative analysis of mRNA expression for infective larvae (L3i) specific transcripts. Quantitative real-time PCR validated the specific expression of six genes in infective L3 larvae. Relative expression of the target genes was assessed by normalizing to 18S rRNA expression. Gene expression in L3i was defined as 1.0. Accession number for genes analysed are as follows: Sv-L3Nie-2; HO652574, Astacin-like metalloprotease; HO652576, SVC L3ist-1 (novel gene); HP429055, SVC L3ist-2 (novel gene); HP429056, *PTC 00570_1*; HP429058, Sv-L3Nie-1; HP429068, FMR Famide-related peptide; HO652180, Poly (A)-binding protein; HO652261.

*S. stercoralis* has failed uncover evidence of an L3i/dauer expression signature conserved between the two species [27].

On the other hand, interesting expression patterns were observed in small heat-shock proteins, Hsp20. We found that infective larvae of *S. venezuelensis* had at least three Hsp20s, which were significantly different not only in the sequence but in the expression pattern along the developmental stages as well (Fig. 3A). In mammals, Hsp20 protects cells from the aggregation of denatured proteins, and is abundantly expressed in smooth muscle cells and cardiomyocytes [28,29]. In parasitic nematodes, small heat-shock proteins have been reported to have a role in muscle cells and muscle contraction [30]. Therefore these Hsp20 might be involved in different muscular functions, or they might have totally different roles in *S. venezuelensis*.

Upon infection, infective larvae must penetrate skin as quickly as possible. Infective larvae of *S. venezuelensis* have a zinc metalloprotease activity, which has been assumed to play a major role in skin penetration [12]. This metalloprotease activity at 40 kDa is presumably a *S. venezuelensis* homologue of Ss40 of *S. stercoralis*, a zinc metalloprotease deployed by infective larvae [31,32]. Recent study identified an astacin-like metalloprotease transcript in infective larvae of *S. stercoralis*, which has been referred to as 'strongylastacin' [33], to which one of the transcripts in the present study (HO652576) is highly homologous. The expression of this transcript is specific for infective larva stage, which perfectly matches to the metalloprotease activity previously reported [12].

The most significant results in this study were that the substantial portion of transcripts of *S. venezuelensis* infective larvae contained novel sequences. Especially, novel transcripts, SVC L3ist-1 and SVC L3ist-2, were abundantly expressed and they were infective larva-specific (Table 5, Fig. 4). We could not find similar sequences in public nucleotide databases, even against NEMABESE4, the most comprehensive resource for nematode EST analysis. Because NEMABESE4 contains EST data on *S. stercoralis* as well as *S. ratti*, these two transcripts should be not only stage-specific but species-specific molecules. Transcriptome analysis of *Ancylostoma caninum* has revealed that more than 80% of infective larva-specific transcripts (66 out of 78) are species-specific [34]. Comparative genomics among hookworms and *Srtongyloides* nematodes, that produce tissue penetrating infective larvae, should be one of the most exciting issues in the field of parasitology.

Apart from the biology of *S. venezuelensis* infective larvae, we could identify transcripts for candidate antigens for immunodiagnosis. We found two different transcripts homologous to *S. stercoralis* L3Nie antigen (SvL3Nie-1 and SvL3Nie-2) and proteinase inhibitor I33, which is similar to *Onchocerca volvulus* immunodominant antigen Ov33 (HP429083). L3Nie antigen is a member of the Ancylostoma Secretory Protein family, which was cloned with a patient serum [35], and has been shown to be useful in the diagnosis of strongyloidiasis [36]. Ov33, on the other hand, is recognized by more than 90% of onchocerciasis patient sera and has been used for immunodiagnosis as a single protein or fusion protein [37,38]. Gold standard for the diagnosis method for strongyloidiasis is the stool examination, however, the sensitivity of detecting larvae is not enough especially for chronic infections in immunocompetent hosts [39,40]. Because Ov33 homologue and L3Nie antigen appear to be abundantly transcribed in larvae, the combined use of the two antigens in immunodiagnosis might improve the sensitivity and specificity

significantly. Therefore further analysis is required of these antigens with strongyloidiasis patient sera.

## 5. Conclusions

A total of 408 EST were obtained from a cDNA library of *S. venezuelensis* infective larvae. Most abundant transcripts are those for lipase, respiration enzymes, and heat-shock proteins, however they contained 37 novel sequences which cannot be found in public nucleotide databases. Of seven transcripts which are infective larvae stage-specific, three have been unannotated and two were novel. Further research on these novel genes will clarify the biology of the infective larva.

## Acknowledgements

This work was supported by grants from the Ministry of Education, Culture, Sports, Science and Technology of Japan (Grant-in-Aid for Scientific Research C 21590466, Grant-in-Aid for Scientific Research on Priority Areas 'Matrix of Infection Phenomena' 21022041), the Ministry of Health, Labour and Welfare (H20-Shinko-Ippan-016, H21-Kokui-Shitei-004), and the Japan Health Sciences Foundation (KHA2031).

## References

[1] Román-Sánchez P, Pastor-Guzmán A, Moreno-Guillén S, Igual-Adell R, Suñer-Generoso S, Tornero-Estébanez C. High prevalence of *Strongyloides stercoralis* among farm workers on the Mediterranean coast of Spain: analysis of the predictive factors of infection in developed countries. Am J Trop Med Hyg 2003;69:336–40.
[2] Safdar A, Malathum K, Rodriguez SJ, Husni R, Rolston KV. Strongyloidiasis in patients at a comprehensive cancer center in the United States. Cancer 2004;100: 1531–6.
[3] Hirata T, Uchima N, Kishimoto K, Zaha O, Kinjo N, Hokama A, et al. Impairment of host immune response against *Strongyloides stercoralis* by human T cell lymphotropic virus type 1 infection. Am J Trop Med Hyg 2006;74:246–9.
[4] Couillault C, Pujol N, Reboul J, Sabatier L, Guichou JF, Kohara Y, et al. TLR-independent control of innate immunity in *Caenorhabditis elegans* by the TIR domain adaptor protein TIR-1, an ortholog of human SARM. Nat Immunol 2004;5: 488–94.
[5] Pujol N, Zugasti O, Wong D, Couillault C, Kurz CL, Schulenburg H, et al. Anti-fungal innate immunity in *C. elegans* is enhanced by evolutionary diversification of antimicrobial peptides. PLoS Pathog 2008;4:e1000105.
[6] Hotez PJ, Bethony J, Bottazzi ME, Brooker S, Diemert D, Loukas A. New technologies for the control of human hookworm infection. Trends Parasitol 2006;22:327–31.
[7] Suarez VH. Helminthic control on grazing ruminants and environmental risks in South America. Vet Res 2002;33:563–73.
[8] De Lange HJ, Lahr J, Van der Pol JJ, Wessels Y, Faber JH. Ecological vulnerability in wildlife: an expert judgment and multicriteria analysis tool using ecological traits to assess relative impact of pollutants. Environ Toxicol Chem 2009;28:2233–40.
[9] Maruyama H, Nawa Y, Ohta N. *Strongyloides venezuelensis*: binding of orally secreted adhesion substances to sulfated carbohydrates. Exp Parasitol 1998;89:16–20.
[10] Korenaga M, Nawa Y, Mimori T, Tada I. *Strongyloides ratti*: the role of enteral antigenic stimuli by adult worms in the generation of protective immunity in rats. Exp Parasitol 1983;55:358.
[11] Maruyama H, Yabu Y, Yoshida A, Nawa Y, Ohta N. A role of mast cell glycosaminoglycans for the immunological expulsion of intestinal nematode, *Strongyloides venezuelensis*. J Immunol 2000;164:3749–54.
[12] Maruyama H, Nishimaki A, Takuma Y, Kurimoto M, Suzuki T, Sakatoku Y, et al. Successive changes in tissue migration capacity of developing larvae of an intestinal nematode, *Strongyloides venezuelensis*. Parasitology 2006;132:1–8.
[13] Wertheim G. Growth and development of *Strongyloides venezuelensis* Brumpt, 1934 in the albino rat. Parasitology 1970;61:381–8.
[14] Gill GV, Welch E, Bailey JW, Bell DR, Beeching NJ. Chronic *Strongyloides stercoralis* infection in former British Far East prisoners of war. Q J Med 2004;97:789–95.
[15] Keiser PB, Nutman TB. *Strongyloides stercoralis* in the immunocompromised population. Clin Microbiol Rev 2004;17:208–17.
[16] Yamaguchi K, Takatsuki K. Adult T cell leukaemia-lymphoma. Baillières Clin Haematol 1993;6:899–915.
[17] Verdonck K, González E, Van Dooren S, Vandamme AM, Vanham G, Gotuzzo E. Human T-lymphotropic virus 1: recent knowledge about an ancient infection. Lancet Infect Dis 2007;7:266–81.
[18] Marcos LA, Terashima A, Dupont HL. Strongyloides hyperinfection syndrome: an emerging global infectious disease. Trans R Soc Trop Med Hyg 2008;102:314–8.
[19] Audic S, Claverie JM. The significance of digital gene expression profiles. Genome Res 1997;7:986–95.
[20] Ashton FT, Zhu X, Boston R, Lok JB, Schad GA. *Strongyloides stercoralis*: amphidial neuron pair ASJ triggers significant resumption of development by infective larvae under host-mimicking in vitro conditions. Exp Parasitol 2007;115:92–7.
[21] Singh R, Kaushik S, Wang Y, Xiang Y, Novak I, Komatsu M, et al. Autophagy regulates lipid metabolism. Nature 2009;458:1131–5.
[22] Mizushima N, Yamamoto A, Matsui M, Yoshimori T, Ohsumi Y. In vivo analysis of autophagy in response to nutrient starvation using transgenic mice expressing a fluorescent autophagosome marker. Mol Biol Cell 2004;15:1101–11.
[23] Kuma A, Hatano M, Matsui M, Yamamoto A, Nakaya H, Yoshimori T, et al. The role of autophagy during the early neonatal starvation period. Nature 2004;432: 1032–6.
[24] Shibata M, Yoshimura K, Tamura H, Ueno T, Nishimura T, Inoue T, et al. LC3, a microtubule-associated protein1A/B light chain3, is involved in cytoplasmic lipid droplet formation. Biochem Biophys Res Commun 2010;393:274–9.
[25] Nollen EA, Morimoto RI. Chaperoning signaling pathways: molecular chaperones as stress-sensing 'heat shock' proteins. J Cell Sci 2002;115:2809–16.
[26] Ogawa A, Streit A, Antebi A, Sommer RJ. A conserved endocrine mechanism controls the formation of dauer and infective larvae in nematodes. Curr Biol 2009;19:67–71.
[27] Mitreva M, McCarter JP, Martin J, Dante M, Wylie T, Chiapelli B, et al. Comparative genomics of gene expression in the parasitic and free-living nematodes *Strongyloides stercoralis* and *Caenorhabditis elegans*. Genome Res 2004;14:209–20.
[28] Fan GC, Ren X, Qian J, Yuan Q, Nicolaou P, Wang Y, et al. Novel cardioprotective role of a small heat-shock protein, Hsp20, against ischemia/reperfusion injury. Circulation 2005;111:1792–9.
[29] Salinthone S, Tyagi M, Gerthoffer WT. Small heat shock proteins in smooth muscle. Pharmacol Ther 2008;119:44–54.
[30] Raghavan N, Ghosh I, Eisinger WS, Pastrana D, Scott AL. Developmentally regulated expression of a unique small heat shock protein in *Brugia malayi*. Mol Biochem Parasitol 1999;104:233–46.
[31] McKerrow JH, Brindley P, Brown M, Gam A, Stanton C, Neva FA. *Strongyloides stercoralis*: identification of a protease that facilitates penetration of the skin by the infective larvae. Exp Parasitol 1990;70:134–43.
[32] Brindley PJ, Gam AL, McKerrow JH, Neva FA. Ss40: the zinc endopeptidase secreted by infective larvae of *Strongyloides stercoralis*. Exp Parasitol 1995;80:1–7.
[33] Gomez Gallego S, Loukas A, Slade RW, Neva FA, Varatharajalu R, Nutman TB, et al. Identification of an astacin-like metallo-proteinase transcript from the infective larvae of *Strongyloides stercoralis*. Parasitol Int 2005;54:123–33.
[34] Wang Z, Abubucker S, Martin J, Wilson RK, Hawdon J, Mitreva M. *Ancylostoma caninum* transcriptome and exploring nematode parasitic adaptation. BMC Genomics 2010;11:307.
[35] Ravi V, Ramachandran S, Thompson RW, Andersen JF, Neva FA. Characterization of a recombinant immunodiagnostic antigen (NIE) from *Strongyloides stercoralis* L3-stage larvae. Mol Biochem Parasitol 2002;125:73–81.
[36] Ramanathan R, Burbelo PD, Groot S, Iadarola MJ, Neva FA, Nutman TB. A luciferase immunoprecipitation systems assay enhances the sensitivity and specificity of diagnosis of *Strongyloides stercoralis* infection. J Infect Dis 2008;198:444–51.
[37] Lucius R, Kern A, Seeber F, Pogonka T, Willenbucher J, Taylor HR, et al. Specific and sensitive immunodiagnosis of onchocerciasis with a recombinant 33 kD *Onchocerca volvulus* protein (Ov33). Trop Med Parasitol 1992;43:139–45.
[38] Nde PN, Pogonka T, Bradley JE, Titanji VP, Lucius R. Sensitive and specific serodiagnosis of onchocerciasis with recombinant hybrid proteins. Am J Trop Med Hyg 2002;66:566–71.
[39] Sato Y, Kobayashi J, Toma H, Shiroma Y. Efficacy of stool examination for detection of *Strongyloides* infection. Am J Trop Med Hyg 1995;53:248–50.
[40] Siddiqui AA, Berk SL. Diagnosis of *Strongyloides stercoralis* infection. Clin Infect Dis 2001;33:1040–7.

# Notch2 signaling is required for proper mast cell distribution and mucosal immunity in the intestine

Mamiko Sakata-Yanagimoto,[1,2] Toru Sakai,[3] Yasuyuki Miyake,[1] Toshiki I. Saito,[2,4] Haruhiko Maruyama,[5] Yasuyuki Morishita,[6] Etsuko Nakagami-Yamaguchi,[2] Keiki Kumano,[2,7] Hideo Yagita,[8] Masashi Fukayama,[9] Seishi Ogawa,[9,10] Mineo Kurokawa,[7] Koji Yasutomo,[3] and Shigeru Chiba[1,2]

[1]Department of Clinical and Experimental Hematology, University of Tsukuba, Tsukuba, Japan; [2]Department of Cell Therapy and Transplantation Medicine, University of Tokyo Hospital, Tokyo, Japan; [3]Department of Immunology and Parasitology, Institute of Health Biosciences, The University of Tokushima Graduate School, Tokushima, Japan; [4]Laboratory of Cell Therapy, Department of Regenerative Medicine, Clinical Research Center, National Hospital Organization Nagoya Medical Center, Nagoya, Japan; [5]Parasitic Diseases Unit, Department of Infectious Diseases, Faculty of Medicine, University of Miyazaki, Miyazaki, Japan; [6]Department of Pathology, University of Tokyo, Tokyo, Japan; [7]Department of Hematology and Oncology, University of Tokyo, Tokyo, Japan; [8]Department of Immunology, Juntendo University School of Medicine, Tokyo, Japan; [9]Cancer Genomics Project, Graduate School of Medicine, University of Tokyo, Tokyo, Japan; and [10]Core Research for Evolutional Science and Technology, Japan Science and Technology Agency, Tokyo, Japan

**Notch receptor-mediated signaling is involved in the developmental process and functional modulation of lymphocytes, as well as in mast cell differentiation. Here, we investigated whether Notch signaling is required for antipathogen host defense regulated by mast cells. Mast cells were rarely found in the small intestine of wild-type C57BL/6 mice but accumulated abnormally in the lamina propria of the small-intestinal mucosa of the *Notch2*-conditional knockout mice in naive status. When transplanted into mast cell–deficient $W^{sh}/W^{sh}$ mice, *Notch2*-null bone marrow-derived mast cells were rarely found within the epithelial layer but abnormally localized to the lamina propria, whereas control bone marrow-derived mast cells were mainly found within the epithelial layer. After the infection of *Notch2* knockout and control mice with L3 larvae of *Strongyloides venezuelensis*, the abundant number of mast cells was rapidly mobilized to the epithelial layer in the control mice. In contrast, mast cells were massively accumulated in the lamina propria of the small intestinal mucosa in *Notch2*-conditional knockout mice, accompanied by impaired eradication of *Strongyloides venezuelensis*. These findings indicate that cell-autonomous Notch2 signaling in mast cells is required for proper localization of intestinal mast cells and further imply a critical role of Notch signaling in the host-pathogen interface in the small intestine. (*Blood*. 2011;117(1):128-134)**

## Introduction

Mast cells are important in a wide variety of physiologic and pathologic processes, including protective immune responses to parasites and allergic disorders.[1,2] In intestinal parasite infection, mast cells play a central role in the immune response.[3] During the induction phase of parasite-induced inflammation, mast cells move from the submucosa to the tip of the villi, accompanying the serial changes in the protease expression pattern. Initially, they are positive for mouse mast cell protease-5 (mMCP-5) but negative for mMCP-1 and mMCP-2; eventually, they become positive for mMCP-1 and mMCP-2 but negative for mMCP-5, demonstrating convergence from connective tissue–type mast cells (CTMCs) to mature mucosal-type mast cells (MTMCs).[4] The parasite-infected mice consequently experience jejunal mast cell hyperplasia,[5] and the serum concentration of mMCP-1, an activation marker of small intestinal mast cells, is increased by > 1000-fold compared with that in the naive status.[5]

In the mammalian immune system, we and other groups have demonstrated that Notch signaling is involved in the commitment and differentiation of T cells, the development of splenic marginal zone B cells, and the differentiation and functional modulation of mature T cells, including T-helper type I (Th1)/Th2 polarization[6,7] and differentiation of CD8-positive cytotoxic T cells.[8] Regarding the Notch signaling in mast cells, bone marrow-derived mast cells (BMMCs) highly express Jagged1[9] and Notch2[10] among the Notch ligands and the receptors, respectively. We have previously shown that signaling through the Notch2 receptor induces mast cell development from myeloid progenitors by transcriptional up-regulation of hairy and enhancer of split homolog-1 (Hes-1) and transacting T cell–specific transcription factor GATA-3 (GATA3).[11] Induction of antigen-presenting potential of mast cells by Notch signaling is also demonstrated.[12] A question yet to be solved is how Notch signaling affects mast cell properties in vivo.

In this report, we examined the effect of Notch2 signaling in in vivo mast cells using *Notch2*-conditional knockout mice.[13] We show that Notch2 signaling is specifically required for intraepithelial localization of intestinal mast cells and antiparasite immunity. In contrast, Notch2 is dispensable for either distribution or development of CTMCs.

Submitted July 9, 2010; accepted September 28, 2010. Prepublished online as *Blood* First Edition paper, October 22, 2010; DOI 10.1182/blood-2010-07-289611.

The online version of this article contains a data supplement.

The publication costs of this article were defrayed in part by page charge payment. Therefore, and solely to indicate this fact, this article is hereby marked "advertisement" in accordance with 18 USC section 1734.

## Methods

### Mice

The generation of *Notch2*$^{flox/flox}$ mice was described previously.[13] Mx-*Cre* transgenic mice[14] were crossed with *Notch2*$^{flox/flox}$ mice (*N2*-MxcKO mice) and the progeny were injected with polyinosinic-polycytidylic acid (pIpC; Sigma-Aldrich) 7 times every other day from 3 days after birth (25 μg/g body weight) or 3 times between 4 and 6 weeks of age (20 μg/g body weight). *N2*-MxcKO mice were further crossed with C57BL/6-Ly5.1 mice (a kind gift from Dr H. Nakauchi, University of Tokyo) to generate Ly5.1-*N2*-MxcKO mice. *Notch2* deletion in bone marrow was examined by polymerase chain reaction and 3% agarose gel electrophoresis[13] (supplemental Figure 1, available on the *Blood* Web site; see the Supplemental Materials link at the top of the online article). *W*$^{sh}$/*W*$^{sh}$ mice were purchased from The Jackson Laboratory. All experiments were done with approval from the University of Tsukuba Institutional Review Board.

### Staining

Sections, fixed with Carnoid fluid, were stained with 0.5% toluidine blue (Sigma-Aldrich), pH 0.3, followed by eosin. Small intestine was embedded in optimal cutting temperature (OCT) compound (TissueTek) and cut with cryostat (Leica CM1850). The section was fixed with 4% paraformaldehyde, washed with phosphate-buffered saline (PBS), blocked in 10% horse serum and 0.1% Triton-PBS, and then stained with either 1:100 goat anti-Jagged1 antibody (C-20; Santa Cruz Biotechnology), goat anti-Delta1 antibody (Genzyme Tech), or control goat immunoglobulin G (IgG; Santa Cruz Biotechnology) overnight at 4°C. The sections were washed with PBS and stained with anti–goat Alexa 594 (Invitrogen). Sections were analyzed by fluorescence microscope (Zeiss; Axioplan2), original magnification ×200.

### BMMCs

Bone marrow cells from each mouse strain were cultured in RPMI 1640 medium (Sigma-Aldrich) supplemented with 10% fetal bovine serum (FBS), 50 ng/mL stem cell factor (SCF; PeproTech), and 10 ng/mL interleukin-3 (IL-3; PeproTech) for 4 weeks. Generation of BMMCs was confirmed by staining with lineage markers, c-Kit and IgE, as previously described.[11] Briefly, the cells were incubated with purified IgE (BD Biosciences) after blocking the Fcγ receptors with purified anti-CD16/32 antibody (BD Biosciences), stained with anti-IgE–fluorescein isothiocyanate (FITC; BD Biosciences), anti–Gr-1–phycoerythrin (PE), anti-Mac1–PE (eBioscience), and anti–c-Kit–allophycocyanin (APC; eBioscience), and then analyzed by FACSCalibur (BD Biosciences).

### Peritoneal mast cells

Five milliliters ice-cold PBS was injected into the peritoneal cavity, and then 3 mL PBS was recovered. c-Kit and IgE receptor (FcεRI) expression was used to define the cells as peritoneal mast cells. Ly5.1 and Notch2 were stained with anti-Ly5.1–PE (BD Biosciences) or biotinylated anti-Notch2 antibody (clone HMN2-35)[8] followed by streptavidin PE (eBioscience), respectively.

### Bone marrow transplantation

C57BL/6 mice and *W*$^{sh}$/*W*$^{sh}$ mice were lethally irradiated with a total dose of 9.5 Gy and then transplanted with $1 \times 10^7$ whole bone marrow cells from either *N2*-MxcKO-Ly5.1 mice or *Notch2*$^{flox/flox}$-Ly5.1 mice from the tail vein. Tissues of transplanted mice were assessed at 3 to 4 months after transplantation. Donor-cell engraftment was assessed by fluorescence-activated cell sorting (FACS) analysis of peripheral blood, which was stained by anti-Ly5.2–FITC (BD Biosciences) and anti-Ly5.1–PE.

### *S venezuelensis* infection

Mice were infected by subcutaneous injection of third-stage infective larvae of *Strongyloides venezuelensis*. The degree of infection was monitored by counting the number of eggs per gram of feces. Mast cells were counted and presented as the number per 10 villus crypt units. BMMCs were washed with PBS twice and then cultured with 10 ng/mL IL-4 and 10 ng/mL IL-10 for 3 days. These Th2-conditioned BMMCs were injected at day 3 and day 6 of experiments.[15] In contrast to the bone marrow transplantation, mice were not irradiated before BMMC injection.

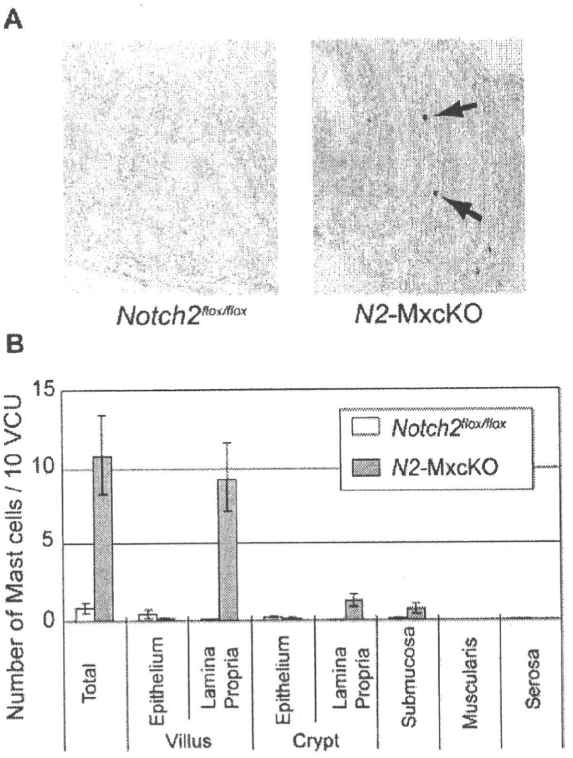


**Figure 1. Mature mast cells were abnormally accumulated in the lamina propria of the small intestine of *Notch2*-deficient mice.** (A) Sections of the small intestine of *N2*-MxcKO or littermate control *Notch2*$^{flox/flox}$ mice. Toluidine blue staining, followed by eosin. Original magnification ×200. (B) The numbers of mast cells per 10 villus crypt units (vcus) distributing to various layers of the small intestine. Data are presented as means ± SEM; *Notch2*$^{flox/flox}$ (n = 10) versus *N2*-MxcKO (n = 8); $P = .000461$ (total), $P = .000261$ (villus, lamina propria), $P = .001918$ (crypt, lamina propria), $P = .046874$ (submucosa).

### Statistical analysis

The data for the number of mast cells and the *S venezuelensis* infection data were analyzed by the *t* test. *P* values < .05 were considered significant.

## Results

### Notch signaling affects the number and localization of mast cells in the small intestine

We have previously reported that Notch2 regulates mast cell differentiation in vitro.[11] To examine whether Notch2 controls the differentiation or development of MTMCs in vivo, we examined intestinal mast cells by toluidine blue staining in C57BL/6 mice carrying the *Notch2*$^{flox/flox}$ allele with or without the Mx1-*Cre* transgene (*N2*-MxcKO mice or *Notch2*$^{flox/flox}$ mice, respectively) after pIpC treatment.[13] Mast cells were only sparsely detected in the small intestine of *Notch2*$^{flox/flox}$ mice, mainly within the epithelium. However, the total number of mast cells in the small intestine of *N2*-MxcKO mice was unanticipatedly greater than that of *Notch2*$^{flox/flox}$ mice. Furthermore, those mast cells were mainly

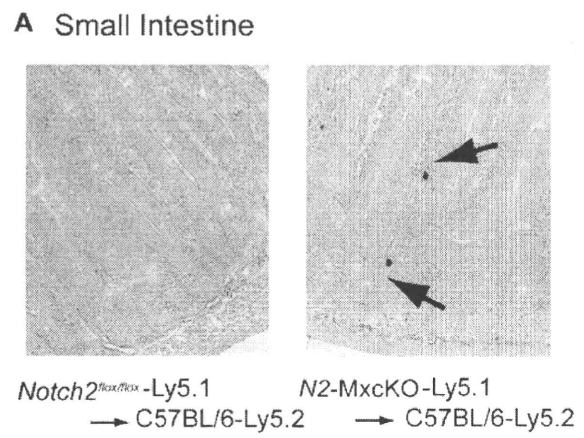


**Figure 2. Localization of intestinal mast cells is abnormal in wild-type mice transplanted with *N2*-MxcKO-Ly5.1 bone marrow cells, reminiscent of that in *N2*-MxcKO mice.** (A) Bone marrow cells from either *N2*-MxcKO- Ly5.1 mice or littermate *Notch2*$^{flox/flox}$- Ly5.1 mice were transplanted into lethally irradiated (9.5 Gy) C57BL/6-Ly5.2 mice. Toluidine blue staining, followed by eosin. Original magnification ×200. (B) The numbers of mast cells per 10 vcus distributing to various layers of the small intestine. Data are presented as means ± SEM; Mast cells in C57BL/6-Ly5.2 mice transplanted with *Notch2*$^{flox/flox}$-Ly5.1 (n = 3) versus *N2*-MxcKO-Ly5.1 (n = 3). $P = .020594$ (total) and $P = .030123$ (villus, lamina propria).

localized to the lamina propria, and very few mast cells were found within the epithelium (Figure 1A-B).

### Localization of MTMCs is abnormal in wild-type mice transplanted with *N2*-MxcKO bone marrow cells, reminiscent of that in *N2*-MxcKO mice

Because the Mx-*Cre*–based conditional knockout system deletes target genes not only in the bone marrow cells but also, albeit partially, in the intestinal cells,[14] there was a possibility that *Notch2* deletion in the intestinal cells was responsible for the distinct distribution pattern or increased number of mast cells in *N2*-MxcKO mice compared with control mice. To exclude this possibility, we transplanted *Notch2*-null bone marrow cells carrying the Ly5.1 marker to irradiated wild-type C57BL/6-Ly5.2 mice. A chimerism of donor-derived Ly5.1-positive fraction accounted for more than 70% in the peripheral blood (data not shown). The recipients of bone marrow cells from *Notch2*$^{flox/flox}$ mice showed that the intestinal mast cell distribution was virtually the same as that in wild-type mice, whereas the recipients of *Notch2*-null bone marrow cells showed an increase in mast cells mainly in the lamina propria in an indistinguishable manner from the *N2*-MxcKO mice (Figure 2A-B). This result indicates that deletion of *Notch2* in bone marrow-derived cells alters the distribution pattern and increases the number of mast cells in the small intestine.

### Notch-ligand expression in the small intestine

Notch signaling is known to be activated through Notch ligand-receptor binding.[16] We examined the expression pattern of Notch ligands in the small intestine with antibodies against Notch ligands Jagged1 and Delta1 and found that the epithelial layer was clearly stained with anti-Jagged1 but not with anti-Delta1 antibody (Figure 3). The staining with the anti-Jagged1 antibody was confined to the surface of epithelial cells, especially at their basal side rather than the apical side (Figure 3). The Jagged1 expression pattern suggests a possibility that Jagged1-Notch2 interaction between the basal side of the epithelial cells and mast cells has an important role for mast cell migration from the lamina propria across the basement membrane toward the epithelium (Figure 3). Furthermore, the ligand-receptor binding itself might contribute to mast cell–epithelial cell adhesion to some extent, based on our observation that *Notch2*-expressing BMMCs attached to the Jagged1-expressing Chinese hamster ovary (CHO) cells, while *Notch2*-null BMMCs did not (supplemental Figure 2).

### *Notch2* is dispensable for the CTMC development and distribution

We next investigated the roles of Notch2 in the development of CTMCs. The localization and the number of CTMCs in the skin and peritoneal cavity were not significantly different between *N2*-MxcKO and littermate *Notch2*$^{flox/flox}$ mice more than 4 weeks after the treatment with pIpC (data not shown). This observation might simply indicate that the Mx-*Cre* system was inefficient in the tissue-resident mast cells, as a great majority of peritoneal

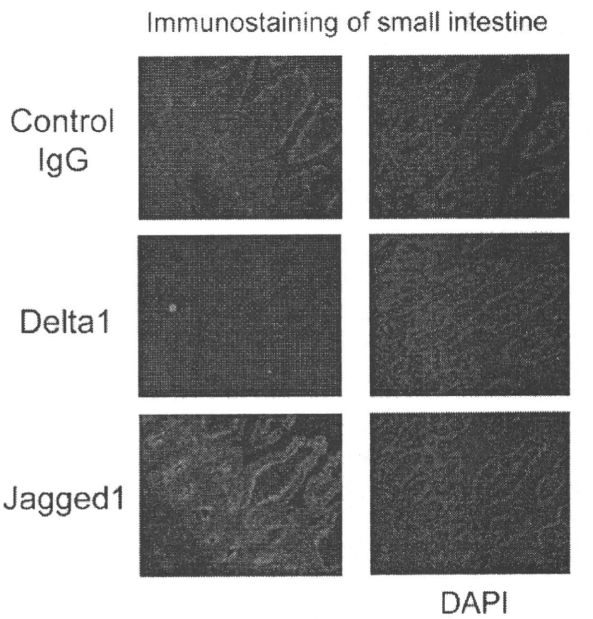


**Figure 3. Jagged1 is strongly expressed on the surface of the epithelial cells, especially at their basal side.** A section of small intestine prepared using cryostat was stained with goat anti-Jagged1 and goat anti-Delta1 antibodies followed by anti–goat Alexa594. Original magnification ×200.

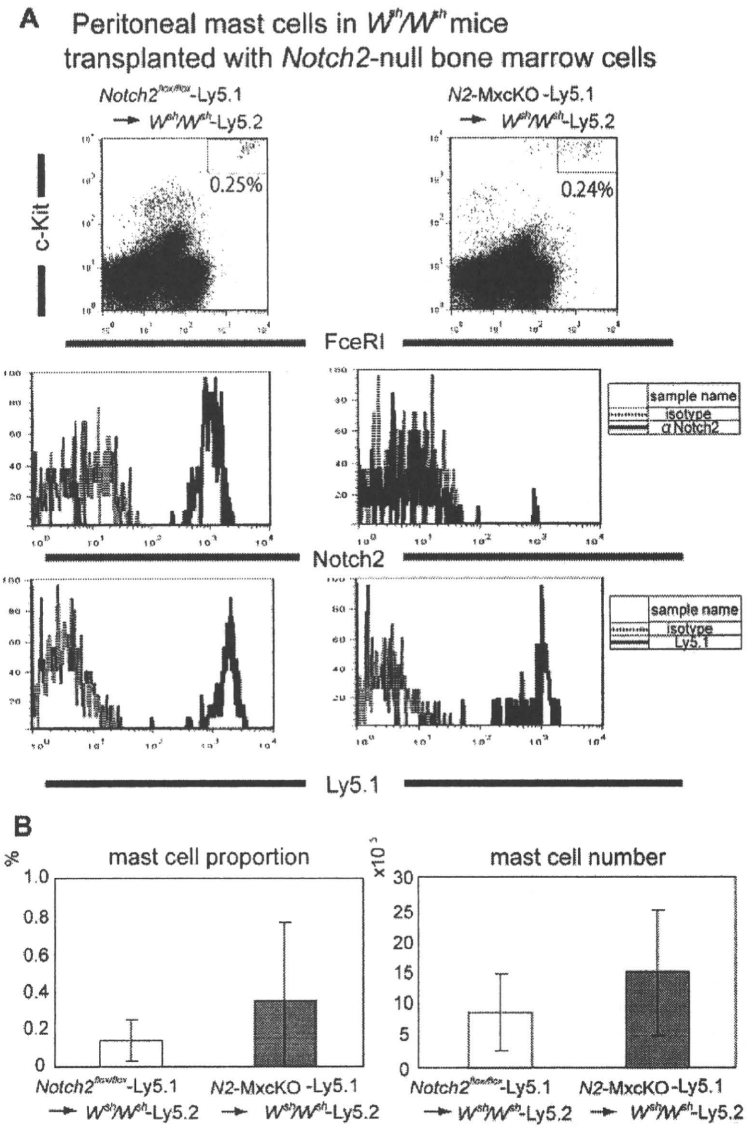


**Figure 4. Notch2 is not required for peritoneal mast cell development.** (A) Bone marrow cells from *N2*-MxcKO-Ly5.1 mice or control *Notch2*$^{flox/flox}$-Ly5.1 mice were transplanted into lethally irradiated *W*$^{sh}$/*W*$^{sh}$ mice. Peritoneal mast cells were stained with anti–c-Kit–APC, IgE, and biotinylated anti-Notch2 antibody (HMN2-35), followed by anti-IgE–FITC and streptavidin-PE, or they were stained with anti–c-Kit–APC, IgE, and anti-Ly 5.1–PE, followed by anti-IgE–FITC; they were then analyzed by FACSCalibur (BD Biosciences). (B) The proportion (left) and the absolute number (right) of peritoneal mast cells were not significantly different between *W*$^{sh}$/*W*$^{sh}$ mice transplanted with *Notch2*-WT bone marrow cells and those transplanted with *Notch2*-null bone marrow cells. $P = .210642$ (mast cell proportion) and $P = .196045$ (mast cell number).

mast cells of pIpC-treated *N2*-MxcKO mice still expressed Notch2 (data not shown). Therefore, to clarify the requirement of *Notch2* in the CTMC development, we examined peritoneal mast cells in mast cell-deficient *W*$^{sh}$/*W*$^{sh}$ mice after transplantion of *Notch2*-null bone marrow cells carrying the Ly5.1 marker. In this system, mast cells exclusively develop from transplanted bone marrow progenitors, in which the *Cre* recombinase under the Mx-promoter is quite effective [14] (supplemental Figure 1). In this experiment, we found that the proportion and absolute number of peritoneal mast cells was not significantly different between those developed from the *N2*-MxcKO-Ly5.1 bone marrow cells and those developed from littermate *Notch2*$^{flox/flox}$-Ly5.1 bone marrow cells (Figure 4A-B). Notch2 was not expressed in the peritoneal mast cells derived from *N2*-MxcKO-Ly5.1 bone marrow cells but was expressed in those derived from littermate *Notch2*$^{flox/flox}$-Ly5.1 bone marrow cells (Figure 4A middle), indicating that *Notch2* was deleted efficiently. These results suggest that Notch2 is dispensable for the development and distribution of CTMCs.

### Cell-autonomous Notch2 signaling in mast cells is important for mast cell migration across the basement membrane in the small intestine

We then asked a question whether aberrant mast cell migration in the small intestine in *N2*-MxcKO mice is dependent on Notch2 signaling in mast cells per se. We intravenously infused *Notch2*-null or control BMMCs into nonirradiated *W*$^{sh}$/*W*$^{sh}$ mice after *S venezuelensis* infection, because it is reported that BMMCs could only transiently reconstitute intestinal mast cells in mast-cell deficient mice if these recipient mice are in naive status.[17] In tissue sections, we found that the distribution of mast cells in the small intestine was different between control BMMCs-reconstituted mice and *Notch2*-null BMMCs-reconstituted mice; control BMMCs were mainly migrated into the epithelial layer, while a majority of *Notch2*-null BMMCs remained in the lamina propria. This observation indicates that mast cell-autonomous Notch2 expression contributes to mast cell migration across the basement membrane from lamina propria into the epithelial layer (Figure 5A-B). Even in the control BMMC-infused mice, however, a substantial proportion of

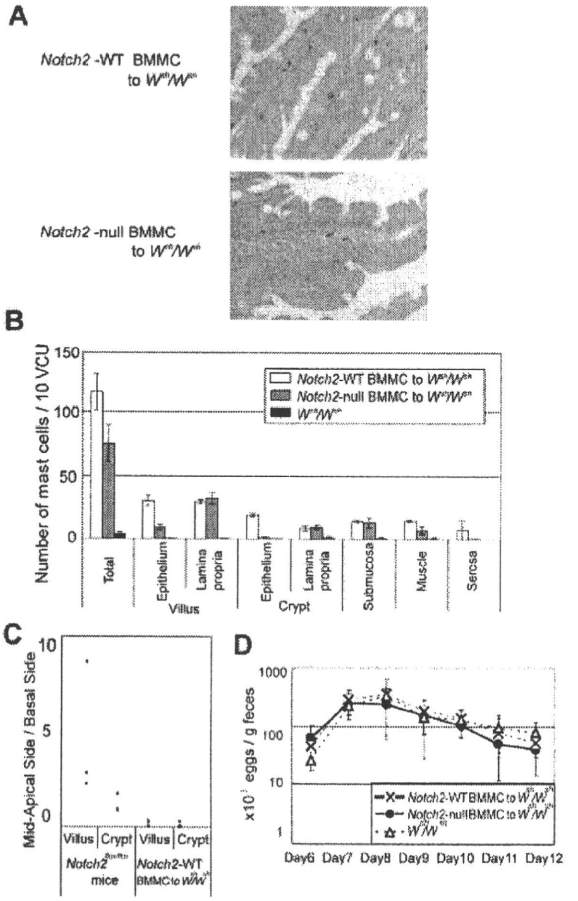


**Figure 5. Mast cell–autonomous Notch2 expression is required for mast cell migration toward the epithelium.** *Wsh/Wsh* mice infected with *S venezuelensis* were intravenously infused with Th2-conditioned *Notch2*-null or control BMMCs on days 3 and 6 of infection. (A) *Notch2*-null BMMCs poorly migrated toward the epithelium compared with control BMMCs. Toluidine blue staining followed by eosin staining. Original magnification ×200. (Top) Control BMMCs; (Bottom) *Notch2*-null BMMCs. (B) The number of mast cells per 10 vcus in the small intestine on day 12 after *S venezuelensis* infection in *Wsh/Wsh* mice, without BMMC infusion, with control BMMC infusion, and with *Notch2*-null BMMC infusion. Data are presented as means ± SEM; n = 3 (control BMMC infusion) and n = 4 (*Notch2*-null BMMC infusion), $P = .004080$ (villus, epithelium) and $P = .000020$ (crypt, epithelium). Note that mast cells in *Wsh/Wsh* mice infused with *Notch2*-null BMMCs abnormally resided in the lamina propria, whereas most of those in *Wsh/Wsh* mice infused with control BMMCs had intraepithelially migrated. (C) Mast cell number in mid to apical side of the epithelial layer was divided with that in the basal side of the epithelial layer. (D) Time course of *S venezuelensis* egg numbers in the stool. The number of excreted eggs was not significantly different between *Wsh/Wsh* mice infused with *Notch2*-null and control BMMCs. Data are presented as means ± SEM.

mast cells still remained in the lamina propria, submucosa, and smooth muscle layers, and the distribution of mast cells within the epithelium was confined to the basement membrane side of the epithelial layer (Figure 5B-C). This mast cell localization pattern was different from that in the *Notch2*$^{flox/flox}$ mice with *S venezuelensis* infection, in which mast cells were present mainly at the mid to apical side of the epithelial layer (Figure 5C). The numbers of *S venezuelensis* eggs in the stool were virtually the same in the *S venezuelensis*–infected *Wsh/Wsh* mice infused with *Notch2*-null and control BMMCs and in the *S venezuelensis*–infected *Wsh/Wsh* mice without any BMMC infusion throughout the period after infection (Figure 5D).

Taken together, the BMMC-*Wsh/Wsh* transplantation model demonstrated that Notch2 in the mast cells indeed determines their intraepithelial migration from lamina propria; nevertheless, this model was not adequate to examine the physiologic mast cell distribution pattern and subsequent parasite expulsion that depends on mast cells.

### Notch2 signaling regulates antiparasite immunity of mast cells in the intestine

The BMMC-*Wsh/Wsh* reconstitution model could not completely reflect physiologic mast cell distribution pattern in the small intestine. Therefore, to further assess the effect of Notch2 signaling on the mucosal immune response of intestinal mast cells under a pathologic condition, *N2*-MxcKO or control *Notch2*$^{flox/flox}$ mice were infected with *S venezuelensis*. Total mast cell number was increased in *Notch2*$^{flox/flox}$ mice much more than in *N2*-MxcKO mice, especially in the epithelium in both crypts and villi 8 days after infection (Figure 6A-B). Thirteen days after infection, mast cells in the epithelium in *Notch2*$^{flox/flox}$ mice were still more abundant than those in *N2*-MxcKO mice (Figure 6C-D), while mast cell accumulation in the lamina propria in *N2*-MxcKO mice was more prominent in both villi and crypt than that in the earlier stage of infection (Figure 6A,C). In particular, dense aggregation of mast cells was prominent in the lamina propria of *N2*-MxcKO mice at the tip of the villi (Figure 6D). As a consequence, the total number of mast cells in the intestine of *N2*-MxcKO mice became equivalent to those of *Notch2*$^{flox/flox}$ mice 13 days after infection (Figure 6C,E). The number of *S venezuelensis* eggs in the stool was gradually decreased during day 8 to 10 in control *Notch2*$^{flox/flox}$ mice but not in *N2*-MxcKO mice (Figure 6F). Furthermore, the worms were still observed in *N2*-MxcKO mice but not in *Notch2*$^{flox/flox}$ mice 12 days after infection (Figure 6G). These data suggest that Notch2 deficiency alters the distinct distribution pattern of mast cells in the small intestine, which is responsible for the defective eradication of *S venezuelensis*.

## Discussion

There is a growing body of evidence that Notch signaling modulates cellular migration and adhesion in endothelial, neural, and lymphoid lineage cells, as well as cancer cells.[18] We have shown that Notch2 signaling induces the development of mast cells.[11] However, it has remained unclear whether Notch2 signaling is involved in the distribution of mast cells in the intestinal mucosa or connective tissues or in controlling the functions of mast cells against microorganisms. Here, we investigated the role of Notch2 signaling in mast cells in terms of their distribution and functions using cell-specific *Notch2*-deficient mice. We found that in *N2*-MxcKO mice, mast cells were abnormally accumulated in the lamina propria of the small intestine, suggesting that *Notch2*-null mast cells have some defect in the migration toward the epithelium. Furthermore, *N2*-MxcKO mice failed to eradicate *S venezuelensis* and exhibited a distinct mast cell migration pattern in the intestine compared with control mice, suggesting that mast cells regulate the host-microbial interface in the intestine through Notch2 signaling.

Mast cell number was rather increased in the intestinal mucosa of *N2*-MxcKO mice compared with control mice in naive status. Mast cell progenitors were supposed to reside in the submucosa and gradually move toward the villi, accompanied by their differentiation into mature mast cells. Based on our observation in

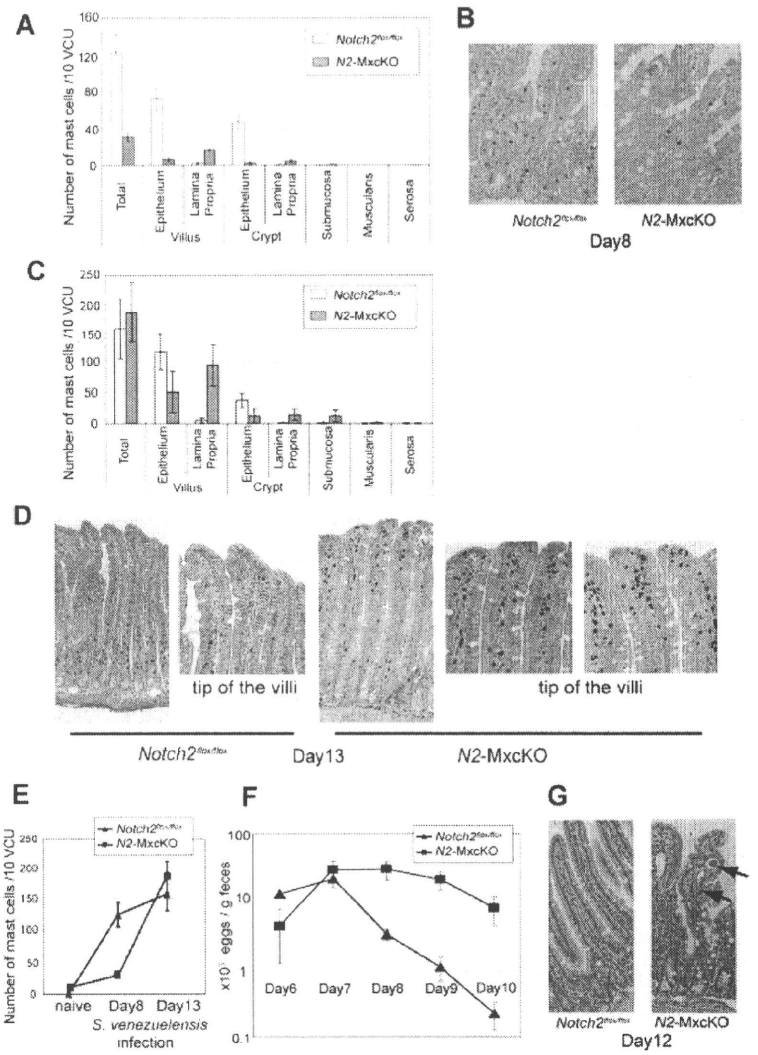


**Figure 6. Notch2 is essential for antiparasite immunity of mast cells in the intestine.** *N2*-MxcKO or control *Notch2*$^{flox/flox}$ mice were subcutaneously injected with third-stage infective larvae of *S venezuelensis*. (A) The number of mast cells per 10 vcus in the small intestine on day 8 after *S venezuelensis* infection. Data are presented as means ± SEM. The number of mast cells was much less in *N2*-MxcKO mice; n = 3, $P = .008592$ (total), $P = .005695$ (villus, epithelium), $P = .000715$ (villus, lamina propria), $P = .005245$ (crypt, epithelium), and $P = .045466$ (crypt, lamina propria). Note that mast cells in *N2*-MxcKO mice were abnormally clustered in the lamina propria, whereas most of those in the control *Notch2*$^{flox/flox}$ mice were intraepithelially migrated. (B) Toluidine blue staining followed by eosin staining of the small intestine on day 8; original magnification ×200. (C) The number of mast cells per 10 vcus in the small intestine on day 13 after *S venezuelensis* infection. Data are presented as means ± SEM; n = 3, $P = .026076$ (villus, epithelium), $P = .00194$ (villus, lamina propria), $P = .021177$ (crypt, epithelium), and $P = .019324$ (crypt, lamina propria), $P = .047445$ (submucosa). (D) Toluidine blue staining followed by eosin staining of the small intestine on day 13. Original magnification ×200. (E) The total number of mast cells per 10 vcus on day 0, day 8, and day 13 of infection. The total number of mast cells was significantly lower in *N2*-MxcKO mice at the early phase (day 8) and almost equal at the later phase (day 13) to that of control mice. Data are presented as means ± SEM; n = 10 and 8 (day 0, *Notch2*$^{flox/flox}$ and *N2*-MxcKO); n = 3 and 3 (day 8, *Notch2*$^{flox/flox}$ and *N2*-MxcKO); n = 4 and 4 (day 13, *Notch2*$^{flox/flox}$ and *N2*-MxcKO). (F) Time course of egg number in the stool. The number of excreted eggs was significantly greater in *N2*-MxcKO mice compared with those in *Notch2*$^{flox/flox}$ mice. Data are represented as means ± SEM; n = 4; $P = .0291$ (day 8) and $P = .0219$ (day 9). (G) Hematoxylin-eosin staining of the small intestine on day 12. Original magnification ×200. Arrows indicate worms. Worms were still observed in the villi in the jejunum of *N2*-MxcKO, but not of *Notch2*$^{flox/flox}$ mice.

an *S venezuelensis*–infection model, mast cells increase in number in the epithelium in control *Notch2*$^{flox/flox}$ mice, while they abnormally aggregate in lamina propria in *N2*-MxcKO mice, especially in the later stage of infection. This suggests that mast cell migration from lamina propria toward the epithelium across the basement membrane is impaired in *N2*-MxcKO mice. Consequently, mast cell turnover might be prolonged in *N2*-MxcKO mice. Given that the mechanism of mast cell migration from lamina propria toward the epithelium is common in naive status and infection status, such migration defect may also explain the mast cell increase in *N2*-MxcKO mice in naive status that we observed.

The defect of mast cell migration toward intraepithelium of the small intestine in *N2*-MxcKO mice is very similar to that in integrin β6-deficient mice,[19] in which activation of transforming growth factor (TGF)–β signaling is impaired.[20] A crosstalk between Notch signaling and TGF-β signaling might occur in intestinal mast cells as well as the cases of other cell types.[21] Alternatively, Notch signaling might directly regulate a downstream target of TGF-β1 in intestinal mast cell migration (eg, the induction of integrin αE expression).[19,22] Integrin αE, forming an integrin αEβ7 complex on mast cells, binds to E-cadherin on epithelial cells and is involved in mast cell localization in the epithelium.[22] The expression level of integrin αEβ7, measured by flow cytometric analysis, however, was not affected by Notch-ligand stimulation in BMMCs (unpublished data).

In the previous paper we showed that Notch signaling facilitates mast cell lineage development at the expense of granulocyte/macrophage development from both common myeloid progenitors (CMPs) and granulocyte-macrophage progenitors (GMPs) in vitro.[11] Mast cells, however, were not depleted in *N2*-MxcKO mice in naive status in vivo, but rather slightly increased in the small intestine of *N2*-MxcKO mice. This clearly indicates that Notch2 signaling is dispensable for steady-state mast cell generation in vivo. However, the dynamic increase of mast cells during the early phase of intestinal parasite infection was markedly impaired in *N2*-MxcKO mice. The mechanisms underlying the Notch2 signaling requirement only in parasite-infected mice remain to be clarified. Nevertheless, rapidly increasing intestinal mast cells have to be supplied by mast cell progenitors. The pathways and mechanisms responsible for mast cell progenitor recruitment and trafficking are likely to be dynamic and susceptible to modification during inflammation.[1] Such a modulation of the mast cell generation pathway during intestinal infection might underlie the requirement of *Notch2* only during parasite infection. This is similar to

IL-3–deficient mice. IL-3 is essential for mast cell differentiation in vitro; however, IL-3–deficient mice have the normal number of mast cells at the steady state, whereas mast cell hyperplasia is impaired upon intestinal parasite infection.[23]

Our data showed that parasite expulsion was impaired in *N2*-MxcKO mice. We could not exclude the possibility that the *Notch2* deletion in immune cells other than mast cells modulate the response against the nematode infection. If we could show that Th2-conditioned wild-type BMMCs successfully eradicate *S venezuelensis* in $W^{sh}/W^{sh}$ mice and that *Notch2*-null BMMCs do not, it would be clearer that Notch2 signaling in mast cells per se but not in other immune cells should be critically important for defense against *S venezuelensis* infection. The failure of rescue experiments may be caused by the abnormal mast cell distribution pattern of wild-type BMMCs in $W^{sh}/W^{sh}$ mice. Nevertheless, the result of this experiment supported the previous finding that the proper epithelial migration of mast cells is required for efficient expulsion of *S venezuelensis*[24] and thus provides an insight that the impaired *S venezuelensis* expulsion in *N2*-MxcKO mice is attributed to the mast cell-autonomous deletion of *Notch2*.

In conclusion, our data clearly indicate that Notch2 receptor signaling is specifically required for proper intestinal mast cell distribution in a cell-autonomous manner. Furthermore, involvement of Notch2 signaling in mucosal immunity was proven, particularly for eradication of infected parasites, although whether this is due to the Notch2 signaling in mast cells is yet to be elucidated.

## Acknowledgments

We thank Dr Shigeo Koyasu for kind advice on the parasite infection experiment and Dr Cliff Takemoto, Dr Eichi Morii, and Dr Keisuke Oboki for kind advice on the histochemistry. We also thank Dr Hiromitsu Nakauchi for the Ly5.1 mice.

This work was supported in part by Grants-in-Aid for Scientific Research from the Japan Society for the Promotion of Science (KAKENHI #21790905 to M.S.-Y. and #18659276 to S.C.) and by grants from Mitsubishi Pharma Research Foundation and Takeda Science Foundation.

## Authorship

Contribution: M.S.-Y. designed and performed the research, analyzed the data, and wrote the paper; T.S., Y. Miyake, and Y. Morishita performed the research; T.I.S., H.M., and H.Y. contributed new reagents; E.N.-Y., K.K., M.F., S.O., and M.K. provided vital discussion; K.Y. designed the research; and S.C. designed the research, analyzed the data, and wrote the paper.

Conflict-of-interest disclosure: The authors declare no competing financial interests.

Correspondence: Shigeru Chiba, Department of Clinical and Experimental Hematology, University of Tsukuba, 1-1-1 Tennodai, Tsukuba, Ibaraki, 305-8575, Japan; e-mail: schiba-tky@umin.net.

## References

1. Gurish MF, Boyce JA. Mast cells: ontogeny, homing, and recruitment of a unique innate effector cell. *J Allergy Clin Immunol.* 2006;117(6):1285-1291.
2. Galli SJ, Nakae S, Tsai M. Mast cells in the development of adaptive immune responses. *Nat Immunol.* 2005;6(2):135-142.
3. Maruyama H, Yabu Y, Yoshida A, Nawa Y, Ohta N. A role of mast cell glycosaminoglycans for the immunological expulsion of intestinal nematode, Strongyloides venezuelensis. *J Immunol.* 2000; 164(7):3749-3754.
4. Friend DS, Ghildyal N, Gurish MF, et al. Reversible expression of tryptases and chymases in the jejunal mast cells of mice infected with Trichinella spiralis. *J Immunol.* 1998;160(11):5537-5545.
5. Miller HR, Pemberton AD. Tissue-specific expression of mast cell granule serine proteinases and their role in inflammation in the lung and gut. *Immunology.* 2002;105(4):375-390.
6. Tsukumo S, Yasutomo K. Notch governing mature T-cell differentiation. *J Immunol.* 2004; 173(12):7109-7113.
7. Radtke F, Wilson A, Mancini SJ, MacDonald HR. Notch regulation of lymphocyte development and function. *Nat Immunol.* 2004;5(3):247-253.
8. Maekawa Y, Minato Y, Ishifune C, et al. Notch2 integrates signaling by the transcription factors RBP-J and CREB1 to promote T-cell cytotoxicity. *Nat Immunol.* 2008;9(10):1140-1147.
9. Singh N, Phillips RA, Iscove NN, Egan SE. Expression of notch receptors, notch ligands, and fringe genes in hematopoiesis. *Exp Hematol.* 2000;28(5):527-534.
10. Jonsson JI, Xiang Z, Pettersson M, Lardelli M, Nilsson G. Distinct and regulated expression of Notch receptors in hematopoietic lineages and during myeloid differentiation. *Eur J Immunol.* 2001;31(11):3240-3247.
11. Sakata-Yanagimoto M, Nakagami-Yamaguchi E, Saito T, et al. Coordinated regulation of transcription factors through Notch2 is an important mediator of mast cell fate. *Proc Natl Acad Sci U S A.* 2008;105(22):7839-7844.
12. Nakano N, Nishiyama C, Yagita H, et al. Notch signaling confers antigen-presenting cell functions on mast cells. *J Allergy Clin Immunol.* 2009; 123(1):74-81 e71.
13. Saito T, Chiba S, Ichikawa M, et al. Notch2 is preferentially expressed in mature B cells and indispensable for marginal zone B lineage development. *Immunity.* 2003;18(5):675-685.
14. Kuhn R, Schwenk F, Aguet M, Rajewsky K. Inducible gene targeting in mice. *Science.* 1995; 269(5229):1427-1429.
15. Fukao T, Yamada T, Tanabe M, et al. Selective loss of gastrointestinal mast cells and impaired immunity in PI3K-deficient mice. *Nat Immunol.* 2002;3(3):295-304.
16. Kopan R, Ilagan MX. The canonical Notch signaling pathway: unfolding the activation mechanism. *Cell.* 2009;137(2):216-233.
17. Tanzola MB, Robbie-Ryan M, Gutekunst CA, Brown MA. Mast cells exert effects outside the central nervous system to influence experimental allergic encephalomyelitis disease course. *J Immunol.* 2003;171(8):4385-4391.
18. Nam DH, Jeon HM, Kim S, et al. Activation of notch signaling in a xenograft model of brain metastasis. *Clin Cancer Res.* 2008;14(13):4059-4066.
19. Brown JK, Knight PA, Pemberton AD, et al. Expression of integrin-alphaE by mucosal mast cells in the intestinal epithelium and its absence in nematode-infected mice lacking the transforming growth factor-beta1-activating integrin alphav-beta6. *Am J Pathol.* 2004;165(1):95-106.
20. Munger JS, Huang X, Kawakatsu H, et al. The integrin alpha v beta 6 binds and activates latent TGF beta 1: a mechanism for regulating pulmonary inflammation and fibrosis. *Cell.* 1999;96(3): 319-328.
21. Kluppel M, Wrana JL. Turning it up a Notch: cross-talk between TGF beta and Notch signaling. *Bioessays.* 2005;27(2):115-118.
22. Wright SH, Brown J, Knight PA, Thornton EM, Kilshaw PJ, Miller HR. Transforming growth factor-beta1 mediates coexpression of the integrin subunit alphaE and the chymase mouse mast cell protease-1 during the early differentiation of bone marrow-derived mucosal mast cell homologues. *Clin Exp Allergy.* 2002;32(2):315-324.
23. Lantz CS, Boesiger J, Song CH, et al. Role for interleukin-3 in mast-cell and basophil development and in immunity to parasites. *Nature.* 1998; 392(6671):90-93.
24. Abe T, Nawa Y. Localization of mucosal mast cells in W/Wv mice after reconstitution with bone marrow cells or cultured mast cells, and its relation to the protective capacity to Strongyloides ratti infection. *Parasite Immunol.* 1987;9(4):477-485.

Parasitology International 59 (2010) 477–480

Contents lists available at ScienceDirect

Parasitology International

journal homepage: www.elsevier.com/locate/parint

Case report

# Zoonotic filariasis caused by *Onchocerca dewittei japonica* in a resident of Hiroshima Prefecture, Honshu, Japan

Shigehiko Uni [a,*], Tomoyuki Boda [b], Koichi Daisaku [b], Yoshihiro Ikura [c], Haruhiko Maruyama [d], Hideo Hasegawa [e], Masako Fukuda [f,g], Hiroyuki Takaoka [g], Odile Bain [h]

[a] *Department of Medical Zoology, Osaka City University Medical School, Abeno-ku, Osaka 545-8585, Japan*
[b] *Shobara Red Cross Hospital, Shobara, Hiroshima 727-0013, Japan*
[c] *Department of Pathology, Osaka City University Medical School, Abeno-ku, Osaka 545-8585, Japan*
[d] *Department of Infectious Diseases, Division of Parasitology, Faculty of Medicine, University of Miyazaki, Miyazaki 889-1692, Japan*
[e] *Department of Biology, Faculty of Medicine, Oita University, Oita 879-5593, Japan*
[f] *Research Promotion Project, Oita University, Oita 879-5593, Japan*
[g] *Department of Infectious Disease Control, Faculty of Medicine, Oita University, Oita 879-5593, Japan*
[h] *Parasitologie comparée, UMR 7205 CNRS, Muséum National d'Histoire Naturelle, 75231 Paris, France*

ARTICLE INFO

*Article history:*
Received 13 May 2010
Accepted 21 May 2010
Available online 31 May 2010

*Keywords:*
Zoonotic onchocerciasis
*Onchocerca dewittei japonica*
Filarioidea
Cuticular characteristics
Wild boar
Japan

ABSTRACT

A female of *Onchocerca* sp. was found to be the probable causative agent of a subcutaneous nodule in the left knee of a 70-year-old man in a rural area of Hiroshima Prefecture, Honshu, the main island of Japan. We compared the characteristics of the agent with the features of the four previously suspected species found in cattle and horses in various parts of the world, as well as *O. lupi* and *O. jakutensis* that were suspected or proved, respectively, in zoonotic cases in Europe. In addition, the morphologic characteristics of this parasite were compared with those of the four *Onchocerca* species found in wild animals in Japan. Based on such characteristics as the large triangle ridges, the considerable distance between any two adjacent ridges, and the absence of inner cuticular striae in the longitudinal sections, we found the causative agent in the present case to be identical to the female of *Onchocerca dewittei japonica*. All five previous cases of zoonotic onchocerciasis in Japan had been found in Oita, Kyushu, the main southern island. This human case caused by *O. dewittei japonica* suggests that zoonotic onchocerciasis is liable to occur in rural areas in Japan where wild boar, *Simulium* vectors, and humans overlap.



## 1. Introduction

Zoonotic filariasis is an infection found in humans which is caused by filarioids of animals [1]. Numerous human cases caused by members of the genus *Dirofilaria* have been found throughout the world [2]. In contrast, human cases caused by *Onchocerca* species parasitic in animals are rare; the first of 15 cases known to date was reported in Ukraine in 1965. Five human cases in Europe, five in Japan, four in North America, and one on the Arabian Peninsula have been discovered worldwide [3–18].

In zoonotic onchocerciasis, the causative agents suspected are *O. gutturosa* Neumann, 1910 from cattle and *O. cervicalis* Railliet and Henry, 1910 from horses [3–8,13]. Much more recently, in Japan, *Onchocerca dewittei japonica* Uni et al., 2001;[19] from wild boar was identified in four of the most recent five cases in Oita, Kyushu, the main southern island of Japan [9,12,14,15]. In retrospect, *O. lupi* found from dogs was suspected to be responsible for subconjunctival infections [3,11] in which the causative agent could not be unambiguously determined in Europe [20]. Finally, *Onchocerca* of the red deer, *O. jakutensis* (Guvanov, 1964) was identified in a patient in Austria [17].

Here we present a new case of a zoonotic onchocerciasis found from a patient living in a rural area of Hiroshima Prefecture in Honshu, the main island of Japan.

## 2. Case study

The patient, a 70-year-old man living in Fuchu City, Hiroshima Prefecture, found a nodule on the left knee in the beginning of the year 2009 and reported feeling pain in the nodule in May 2009. The nodule, 2 cm in diameter, was surgically removed from the subcutaneous connective tissue at the knee at the Shobara Red Cross Hospital in Hiroshima Prefecture in July 2009. The mass excised (1×2 cm) was fixed in 4% paraformaldehyde for 24 h and embedded in paraffin, a routine process. The sections were stained with hematoxylin and eosin. Histologic sections examined: S3-1, S3-2, S3-4, and S7-9.

A coiled worm was found in the nodule and several longitudinal, oblique, and transverse sections of the main part of the body (midbody) of the worm were examined with a microscope (Fig. 1; 1–5). The worm

* Corresponding author. Tel.: +81 6 66453760; fax: +81 6 66453762.
*E-mail address:* uni@med.osaka-cu.ac.jp (S. Uni).

1383-5769/$ – see front matter © 2010 Elsevier Ireland Ltd. All rights reserved.
doi:10.1016/j.parint.2010.05.006

was a female with its uteri in which microfilariae or embryos were not seen (Fig. 1; 1 and 4). In addition, a section of the thin anterior part, 83 μm wide, with the esophagus and a section of the posterior part of the worm, 125 μm wide, were found. Thus, this nodule was occupied by one female adult.

In the longitudinal sections of the worm (Fig. 1; 2), the external transverse ridges were salient on the cuticle and the distance between two adjacent ridges in the main body is shown in Table 1. Our examination revealed two adjoining ridges of one side indicated by two arrows; an arrowhead indicated a small overlapping ridge of the other side (Fig. 1; 2). The distance between the ridges was therefore measured on the ridges of the one side. The ridges formed a sharp triangle (Fig. 1; 3). The cuticle was divided into two main parts of equal thickness and no inner striae were found on the middle line (Fig. 1; 3).

In the transverse sections of the main body, the cuticle was composed of four layers, the muscle cells were 42–52 in number, and the two lateral chords were large. No inner projections of the cuticle were found at the lateral chords. The transverse sections of the midbody were round and lateral thickening of the cuticle was not seen (Fig. 1; 4). The differences of the thickness of the cuticle can be seen at the ridge in Fig. 1; 5. The difference (30 μm) between the thick cuticle (55 μm) and the thin cuticle (25 μm) corresponded to the height of the ridges of *O. dewittei japonica* (Table 1).

Regarding the histologic reaction of the host, the worm was surrounded with eosinophilic exudate in the center of the granuloma while away from the center, macrophages, neutrophils, eosinophils, and lymphocytes had infiltrated the granulomatous tissue (Fig. 1; 1). Macrophages and eosinophils intensively accumulated around some sections of disintegrating parts of the worm (Fig. 1; 5) but neutrophils were very scarce.

The patient, a farmer, lives in a rural area near mountains inhabited by wild boar. He has never been outside Japan and had not visited Oita, Kyushu, within the past several years. He has not raised pets such as

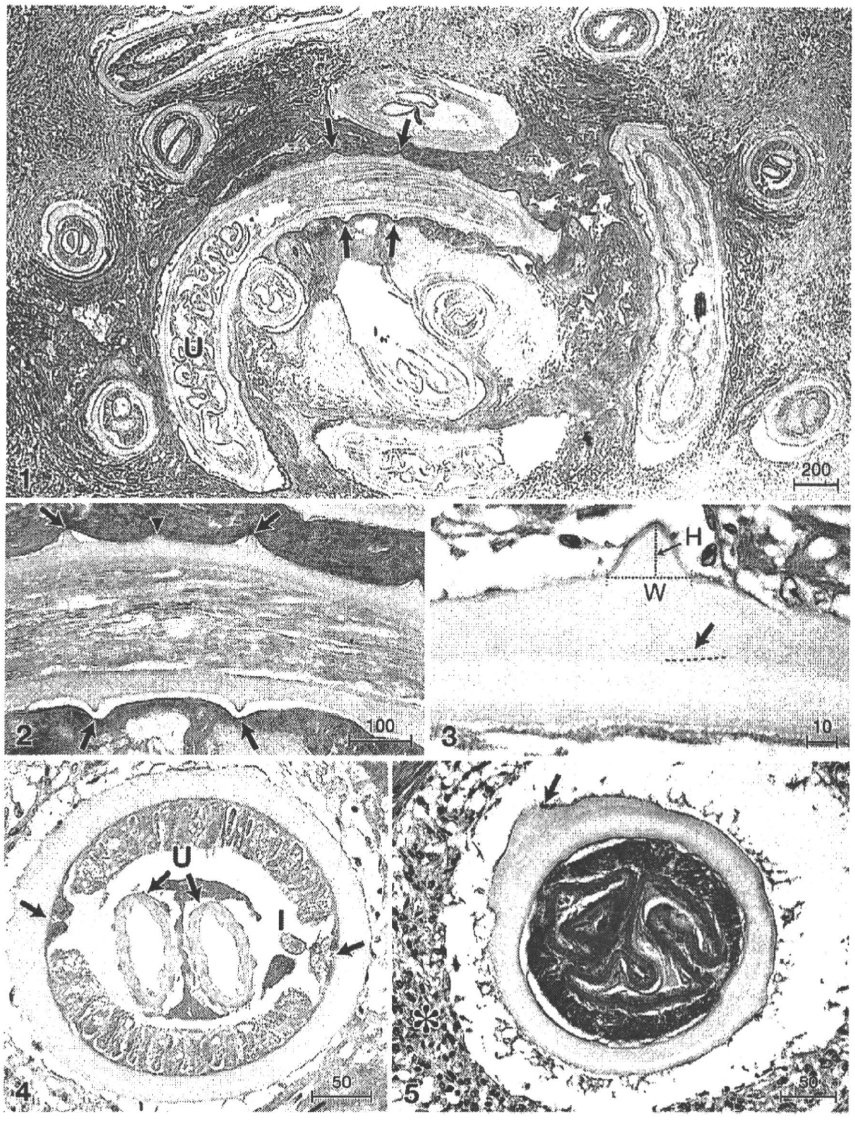


**Fig. 1.** Histologic sections of a female *Onchocerca dewittei japonica*, found in a nodule excised from the left knee of a 70-year-old man. The sections are stained with hematoxylin and eosin. Bars, micrometers. 1. A coiled female with transverse ridges (arrows) on the cuticle and the uteri (U) in the pseudocoelom. 2. The salient transverse ridges (arrows) of one side and a small ridge (an arrowhead) of the other side (semicircular ridges are overlapping at the lateral field, see text). 3. The triangle ridge in the longitudinal section: height (H) and width (W), and the lack of the inner striae at the dotted line with an arrow in the cuticle. 4. The transverse section at the midbody with thick cuticle, muscle cells, and two large lateral chords (arrows). Two empty uteri (U) and intestine (I) in the pseudocoelom. 5. In the transverse section, a thick portion of the cuticle indicates the ridge (an arrow). The section is intensively surrounded by macrophages (*).

**Table 1**
Comparison of histologic characteristics of *Onchocerca* sp. found from a human nodule with females of *Onchocerca* species known in Japan.

| | *Onchocerca* sp. (present study) | *O. gutturosa* | *O. lienalis* | *O. skrjabini* | *O. eberhardi* | *O. suzukii* | *O. dewittei japonica* |
|---|---|---|---|---|---|---|---|
| Body width at midbody | 270–310 | 170–250**, 140–225***, 200–300***** | 180–200**,180–220****, 150–220***** | 170–300 | 60–170 | 228–430 | 180–310 |
| Distance between 2 adjacent ridges | 210–280 | 50–75**, 70–80***, 87–166***** | 30–40**, 25–45****, 60***** | 48–55 | 25–40 | No ridges | 185–290 |
| Shape of ridges (H/W)* in longitudinal sections | Triangle (13–25/23–28) | Rounded ridges (5/12**, 4–5/5–10***, 10–13/26*****) | Small, rounded ridges (3/15–23*****) | Small ridges (6/12) | Small, rounded ridges (3/8) | No ridges | Triangle (8–23/23–30) |
| Thickness of cuticle without ridges | 30–40 | 30**, 25–35*** | 12–17****, 10***** | 20–30 | 28–32 | 15–50 | 10–32 |
| Number of inner striae between 2 adjacent ridges | None | 3**, 4–8***, 2–4***** | 2**, ****, ***** | 3–4 | 2 | None | None |
| Size of lateral chords (H/W)* in transverse sections | 13–25/42–55 | 13/54**** | 16–21/52–63**** | 15–25/50–88 | 10/38 | 5–37/125–132 | 10–18/45–63 |
| Number of muscle cells per quadrant | 8–15 | 2–4**** | 5–7****** | 2–3 | 1–2 | 8–13 | 8–22 |
| Height of muscle cells | 38–43 | 40**** | 31**** | 25–40 | 15–18 | 30–38 | 45–50 |
| Diameter of intestine | 15–18 | 20–34**** | 26**** | 38–68 | 15–20 | 20–48 | 15–17 |
| Host(s) | Human | Cattle | Cattle | Deer and serows | Deer | Serows | Wild boar |
| Histologic sections and references | Sections (S3-1, S3-2, S3-4, S7-9) from a human | **[5]; ***[22]; ****[23]; *****[24] | **[5]; ****[23]; ***** [24]; ******[14] | Sections (YG2-31) from a serow | Sections (S57-F3) from a deer | Sections (YG2-35) from a serow | Sections (B57-1) from a wild boar |

Dimensions in micrometers.
*H/W: height/width.

dogs and cats. Immunologic deficiency was not found in his laboratory examination at the hospital.

## 3. Discussion

In the longitudinal sections, the presence of the transverse ridges on the cuticle of the worm appeared to be typical of a female of the species among the genus *Onchocerca*: 28 species and one subspecies (*O. dewittei japonica*) with the ridges on the cuticle of the female worms and three species without the ridges [21].

The present causative agent can be distinguished from *O. gutturosa* and *O. lienalis*, the two species found in cattle. In these species, the ridges (evident in the posterior part in *O. lienalis*) are rounded, not triangular; the distance between adjacent ridges is smaller; and the females possess inner striae in the cuticle (Table 1), [5,22–24]. In addition, the female of *O. lienalis* has fine, irregular longitudinal striations on the outer surface [23]. The females of *O. cervicalis* and *O. reticulata* from horses have the inner striae in the cuticle and shorter distance between adjoining ridges than that of the causative agent [22]. These four *Onchocerca* species from domestic animals can therefore be excluded from consideration as the causative agent in this case.

The present agent was distinguished from *O. lupi* and *O. jakutensis* in such characteristics as the distance between ridges, the shapes of the ridges, and the inner striae [20,25].

To compare the causative agent with the *Onchocerca* species already found from wild ungulates in Japan, we used portions of the collections of the histologic sections made from females of *Onchocerca* species in the Department of Medical Zoology, Osaka City University Medical School (Table 1) and published descriptions of these species. In Table 1, *O. skrjabini* Rukhlyadev, 1964, taken from a serow, is distinguished from the present human-case causative agent, owing to great differences in such principal characteristics as the distance between adjacent ridges, shape of the ridges, and the inner striae in the cuticle [26,27]. *Onchocerca eberhardi* Uni et al., 2007 taken from a sika deer differs from the causative agent in the diameter of the midbody as well as such characteristics as the distance between the ridges, the shape of ridges, and the inner striae [21]. In *O. suzukii* Yagi et al., 1994 taken from a serow, the transverse ridges are absent on the cuticle [27].

On the contrary, *O. dewittei japonica* taken from a wild boar was found to be identical to the present human-case causative agent in the distance between adjacent ridges, the shape of the ridges, the lack of inner striae in the cuticle, and other dimensions such as the body width, number of muscle cells, and size of lateral chords (Table 1) [19]. Therefore, comparison of the causative agent of the human case with the *Onchocerca* species, either outside Japan or present in Japan, indicated that the agent was a female adult of *O. dewittei japonica*.

Detailed examinations of the histologic sections of *O. dewittei japonica* found both in a human (the present study) and from wild boar now allow us to identify retrospectively this species as the causative agent of the first human case in Japan [7,8] which had been suspected as *O. gutturosa* or *O. cervicalis*. Uni et al. [19] described the ridges of *O. dewittei japonica* female as semicircular, with double thickness of the cuticle on the transverse sections. Thus, the difference in the cuticular thickness has a specific value to suggest the presence of salient ridges in transverse sections. In the slightly oblique section shown in their Fig. 3 of the first human case [7], it is our consideration that the difference (24 μm) between the thick cuticle (36 μm) (with the transverse ridge) and the thin cuticle (12 μm) (without ridges) corresponds to the height (8–23 μm) of ridges on *O. dewittei japonica* rather than that (4–13 μm) of those on *O. gutturosa* (Table 1). The difference in the cuticular thickness therefore indicates that the causative agent in the first human case found was *O. dewittei japonica* also, but this species had not yet discovered from wild boar at that time.

*Wolbachia* bacterial endosymbionts were found in *O. dewittei japonica* [28, Casiraghi et al., ongoing work]. It is indicated that (1) *Wolbachia* stimulate neutrophil infiltration in onchocercomata caused by *Wolbachia*-positive filariae and that (2) eosinophils accumulate to kill the parasites after elimination of the *Wolbachia* by antibiotics [29,30]. Histologic examination showed that, rather than neutrophils, macrophages and eosinophils were abundant around the sections of the worm. The endosymbionts appear to have been destroyed in the altered parts of

the worm; the neutrophils appear to have already been replaced with eosinophils in the course of the death of the parasite in the immunological environment.

Until now, all four known cases of zoonotic onchocerciasis caused by *O. dewittei japonica* parasites found in wild boar (plus probably an earlier case, examined in retrospect) were limited only to Oita, Kyushu. However, the present findings indicate that zoonotic onchocerciasis has occurred in at least one other island of Japan as well. The prevalence of *O. dewittei japonica* in wild boar, as measured by the presence of microfilariae in skin snips, was high in and near Hiroshima Prefecture: 78% (31/40) of wild boar were found to harbor this filarioid in Shimane Prefecture adjoining Hiroshima Prefecture, examined between 2005 and 2006, and was close to the prevalence of the parasites (40/45, or 89%) in wild boar in Oita, Kyushu, in 2003. In Wakayama Prefecture, located in the west-central part of Honshu, 77% (23/30) of wild boar harbored this filarioid in 2007. Thus, as in Kyushu, almost all wild boar over one year old in the western part of Honshu examined, were found to harbor *O. dewittei japonica* (Uni et al., unpublished data).

Having obtained experimentally the infective larvae of *O. dewittei japonica* from several kinds of black flies [31], and having identified as *O. dewittei japonica* the larvae from black flies caught in Oita, Fukuda et al. suggested that *Simulium bidentatum* is a vector in the transmission of the zoonotic onchocerciasis caused by *O. dewittei japonica* in Oita [32]. The black fly inhabits Honshu and Shikoku as well as Kyushu and bites both animals and humans. In the present case, DNA sequences of the mitochondrial *CO1* gene obtained from the causative agent, embedded in paraffin for histologic examination, showed high similarities to those of *O. dewittei japonica* [33, Fukuda et al., in preparation].

In Japan, the habitat of the wild boar (estimated population: several hundred thousands) has recently broadened in the western part of Honshu, Shikoku, and Awaji-shima Island as well as Kyushu, because the annual snowfall has decreased, rice fields left unused by migration of segments of the work forces away from rural areas are favorable habitat for wild boar, and the population of hunters has largely decreased [34]. Therefore, the present human-host case caused by *O. dewittei japonica* suggests that zoonotic onchocerciasis is now liable to occur in other rural areas in Japan, or wherever wild boar and humans are in close proximity and the *Simulium* vectors are known, as well as in Oita.

## Acknowledgements

We thank Prof. Kenichi Wakasa, Department of Diagnostic Pathology, Osaka City University Medical School, for comments about the histologic sections of the human case. We thank Mr. J. L. Yohay for reading the manuscript.

## References

[1] Orihel T, Eberhard ML. Zoonotic filariasis. Clin Microbiol Rev 1998;11:366–81.
[2] Pampiglione S, Rivasi F. Human dirofilariasis due to *Dirofilaria* (*Nochotiella*) *repens*: an update of world literature from 1995 to 2000. Parassitologia 2000;42:231–54.
[3] Azarova NS, Miretsky OY, Sonin MD. The first instance of detection of nematode *Onchocerca* Diesing, 1841 in a person in the USSR. Med Parazitol (Mosk) 1965;34: 156–8 (In Russian).
[4] Siegenthaler R, Gubler R. Paraarticuläres Nematodengranulom (einheimische *Onchocerca*). Schweiz Med Wochenschr 1965;95:1102–4.
[5] Beaver PC, Horner GS, Bilos JZ. Zoonotic onchocercosis in a resident of Illiois and observations on the identification of *Onchocerca* species. Am J Trop Med Hyg 1974;23:595–607.
[6] Ali-Khan Z. Tissue pathology and comparative microanatomy of *Onchocerca* from a resident of Ontario and other enzootic *Onchocerca* species from Canada and the U.S.A. Ann Trop Med Parasitol 1977;71:469–82.
[7] Beaver PC, Yoshimura H, Takayasu S, Hashimoto H, Little MD. Zoonotic *Onchocerca* in a Japanese child. Am J Trop Med Hyg 1989;40:298–300.
[8] Hashimoto H, Murakami I, Fujiwara S, Takayasu S, Takaoka H, Uga S, et al. A human case of zoonotic onchocerciasis in Japan. J Dermatol 1990;17:52–5.
[9] Takaoka H, Bain O, Tajimi S, Kashima K, Nakayama I, Korenaga M, et al. Second case of zoonotic *Onchocerca* infection in a resident of Oita in Japan. Parasite 1996;3: 179–82.
[10] Burr Jr WE, Brown MF, Eberhard ML. Zoonotic *Onchocerca* (Nematoda: Filarioidea) in the cornea of a Colorado resident. Ophthalmology 1998;105:1494–7.
[11] Pampiglione S, Vakalis N, Lyssimachou A, Kouppari G, Orihel TC. Subconjunctival zoonotic *Onchocerca* in an Albanian man. Ann Trop Med Parasitol 2001;95: 827–32.
[12] Takaoka H, Bain O, Uni S, Korenaga M, Tada K, Ichikawa H, et al. Human infection with *Onchocerca dewittei japonica*, a parasite from wild boar in Oita, Japan. Parasite 2001;8:261–3.
[13] Wright RW, Neafie RC, McLean M, Markman AW. Zoonotic onchocerciasis of the shoulder: a case report. J Bone Joint Surg 2002;84:627–9.
[14] Takaoka H, Bain O, Uni S, Korenaga M, Kozek WJ, Shirasaka C, et al. Zoonotic onchocerciasis caused by a parasite from wild boar in Oita, Japan. A comprehensive analysis of morphological characteristics of the worms for its diagnosis. Parasite 2004;11:285–92.
[15] Takaoka H, Yanagi T, Daa T, Anzai S, Aoki C, Fukuda M, et al. An *Onchocerca* species of wild boar found in the subcutaneous nodule of a resident of Oita, Japan. Parasitol Int 2005;54:91–3.
[16] Sallo F, Eberhard ML, Fok E, Baska F, Hatvani I. Zoonotic intravitreal *Onchocerca* in Hungary. Ophthalmology 2005;112:502–4.
[17] Koehsler M, Soleiman A, Aspöck H, Auer H, Walochnik J. *Onchocerca jakutensis* filariasis in humans. Emerg Infect Dis 2007;13:1749–52.
[18] Hira PR, Al-Buloushi A, Khalid N, Iqbal J, Bain O, Eberhard ML. Case report: zoonotic filariasis in the Arabian Peninsula: autochthonous onchocerciasis and dirofilariasis. Am J Trop Med Hyg 2008;79:739–41.
[19] Uni S, Bain O, Takaoka H, Miyashita M, Suzuki Y. *Onchocerca dewittei japonica* n. subsp., a common parasite from wild boar in Kyushu Island, Japan. Parasite 2001;8:215–22.
[20] Sréter T, Széll Z, Egyed Z, Varga I. Subconjuncival zoonotic onchocerciasis in man: aberrant infection with *Onchocerca lupi*? Ann Trop Med Parasitol 2002;96: 497–502.
[21] Uni S, Bain O, Agatsuma T, Harada M, Torii H, Fukuda M, et al. *Onchocerca eberhardi* n. sp. (Nematoda: Filarioidea) from sika deer in Japan; relationships between species parasitic in cervids and bovids in the Holarctic region. Parasite 2007;14: 199–211.
[22] Bain O. Redescription de cinq espèces d'onchocerques. Ann Parasitol Hum Comp 1975;50:763–88.
[23] Bain O, Petit G, Poulain B. Validité des deux espèces *Onchocerca lienalis* et *O. gutturosa*, chez les bovins. Ann Parasitol Hum Comp 1978;53:421–30.
[24] Eberhard ML. Studies on the *Onchocerca* (Nematoda: Filarioidea) found in cattle in the United States. I. Systematics of *O. gutturosa* and *O. lienalis* with a description of *O. stilesi* sp. n. J Parasitol 1979;65:379–88.
[25] Demiaszkiewicz AW. Redescription of *Onchocerca jakutensis* (Gubanov, 1964) (Nematoda, Filaroidea). Acta Parasitol 1993;38:124–7.
[26] Uni S, Suzuki Y, Katsumi A, Kimata I, Iseki M, Bain O. Taxonomy and pathology of filarial parasites from Japanese serows (*Capricornis crispus*). Proc 9th Int Cong Parasitol; 1998. p. 681–4.
[27] Yagi K, Bain O, Shoho C. *Onchocerca suzukii* n. sp. and *O. skrjabini* (= *O. tarsicola*) from a relict bovid, *Capricornis crispus*, in Japan. Parasite 1994;1:349–56.
[28] Bain O, Casiraghi M, Martin C, Uni S. The Nematoda Filarioidea: critical analysis linking molecular and traditional approaches. Parasite 2008;15:342–8.
[29] Brattig NW, Büttner DW, Hoerauf A. Neutrophil accumulation around *Onchocerca* worms and chemotaxis of neutrophils are dependent on *Wolbachia* endobacteria. Microbes Infect 2001;3:439–46.
[30] Nfon CK, Makepeace BL, Njongmeta LM, Tanya VN, Bain O, Trees AJ. Eosinophils contribute to killing of adult *Onchocerca ochengi* within onchocercomata following elimination of *Wolbachia*. Microbes Infect 2006;8:2698–705.
[31] Fukuda M, Takaoka H, Uni S, Bain O. Infective larvae of five *Onchocerca* species from experimentally infected *Simulium* species in an area of zoonotic onchocerciasis in Japan. Parasite 2008;15:111–9.
[32] Fukuda M, Otsuka Y, Uni S, Bain O, Takaoka H. Molecular identification of infective larvae of three species of *Onchocerca* found in wild-caught females of *Simulium bidentatum* in Japan. Parasite 2010;17:39–45.
[33] Fukuda M, Uni S, Boda T, Daisaku K, Hasegawa H, Otsuka Y, et al. A case of zoonotic onchocerciasis in Hiroshima: identification of the causative agent by mitochondrial DNA analysis of paraffin-embedded specimens. Med Entomol Zool 2010;61: 62 (Suppl.).
[34] Kodera Y. *Sus scrofa* Linnaeus, 1758. In: Ohdachi SD, Ishibashi Y, Iwasa MA, Saitoh T, editors. The wild mammals of Japan. Kyoto: Shoukadoh; 2009. p. 304–5.

寄生虫の標的臓器別症状からすすめる実地診療
—疑い，問診・診断から治療まで—

# 腹部症状(腹痛，下痢，下血など)

丸山治彦
宮崎大学医学部感染症学講座寄生虫学分野／まるやま・はるひこ

## はじめに●

いわゆる「感染性胃腸炎」の中に占める寄生虫感染症の割合は低いが，寄生虫の側から考えると，消化管はもっとも広く採用されている寄生部位である．回虫，蟯虫，鞭虫，赤痢アメーバやクリプトスポリジウムなどすべて消化管寄生虫である．消化管に一定数以上の虫がいれば何らかの腹部症状が現れる．

症状あるいは訴えが直接的かつ特徴的なときは，それだけで寄生虫を言い当てることも可能なことがある．例えば「排便時にお尻から虫が出てきた．引っ張ったら千切れた」とか「お尻からミミズのような虫が出てきた」などというものである．前者は広節(日本海)裂頭条虫，後者は回虫の可能性が高い．しかしながら，通常の診療では「これはひょっとして寄生虫か」と途中で疑い出すことのほうが多いであろう．本項では，どういうときに寄生虫のことを思い出すべきかに焦点を当てる．

なお，マラリアでも悪心，嘔吐，下痢，腹痛などの腹部症状を訴えることがあるが，これは「発熱」の項目で詳述されるので本項では述べない．

## 寄生虫の種類●

寄生虫の種類自体は膨大な数に上るが，外来で遭遇するであろう消化管関連の寄生虫に絞ればそれほど多いものではない．消化管および肝臓に病変をもたらす寄生虫の種類を**表1**にまとめた．以下に述べるとおり症状は寄生部位に依存するので，主な寄生部位を知っておくと整理しやすい．

注意すべきは，ヒト体内では成熟できずに幼虫が腸管外を移動する，いわゆる幼虫移行症のカテゴリーに含まれる寄生虫も消化管に障害を引き起こす可能性があることである(後述)．

## 寄生虫による腹部症状●

腹痛，下痢，下血などの症状は，寄生虫が消化管やその近傍に寄生して，機械的刺激や炎症反応などの刺激を起こすことが原因である．寄生数が少なければ症状はほとんどないが，虫体が大きい場合などでは少数寄生でも発症しうる．寄生虫は種によって決まった部位に寄生するので，臨床症状から寄生虫の種類を大まかに推定することは可能で，診断の出発点になる．

### 1. 急激に発症する腹痛

上部消化管に寄生虫が存在して急な痛みで発症する場合がある．もっとも代表的なのは胃アニサキス症である．典型的には，夕食に新鮮なサバやイカを食べたところ，夜中に突然心窩部が差し込むように激しく痛み出して寝ていられなくなったという経過をとる．届出数は少ないが，毎年2,000～3,000例くらい発生していると推定されており，夜間の当直で遭遇する可能性が高い．内視鏡による虫体の摘出が診断と治療を兼ねる．

他に上部消化管で急性の痛みを引き起こすものに回虫がある．現代日本で回虫の生活環が維持されているとは思えないが，患者は存在する．回虫は狭いところにもぐり込む性質があるので，胆管に入り込んで胆管を閉塞させ急性胆嚢炎を起こす．この場合，腹部超音波検査で回虫が胆管内の異物として認められる．

その他の例として，幼虫移行症による炎症性腸閉塞がある．ドロレス顎口虫や旋尾線虫タイプXが消化管の腹膜側から組織に侵入し，激しい好酸球性炎症を起こして機能的イレウスに陥る．一般に，寄生虫感染による顕著な好酸球増多は，寄生虫(原虫を除く)の幼虫が腸管外の組織を移行しているときか，成虫が腸管外に寄生しているときにみられる．したがって，著明な好酸球増多があって腹部症状を訴えるときは，腸管外の寄生虫が腹


0910-1551/10/ ¥100/頁 /JCOPY

- マラリアでも悪心，嘔吐，下痢，腹痛などの腹部症状を訴えることがある．
- 著明な好酸球増多があって腹部症状を訴えるときは，腸管外の寄生虫が腹部症状の原因になっていることを考える．

表1　病変部位別寄生虫リスト

| 寄生部位 | 寄生虫 | 主な症状 | 主な診断方法 | 国内感染 |
|---|---|---|---|---|
| 胃 | アニサキス | 急な胃痛 | 虫体確認 | ＋ |
| 肝―胆道 | ランブル鞭毛虫 | 下痢・腹痛 | 便検査(シスト，栄養体) | ＋ |
| | 赤痢アメーバ(肝膿瘍) | 季肋部痛・発熱 | 抗体検査 | ＋ |
| | 肝蛭 | 季肋部痛・発熱 | 抗体検査 | ＋ |
| | 腸管住血吸虫(虫卵) | 肝機能障害 | 抗体検査・便検査(虫卵) | － |
| | 単包虫 | 季肋部痛・発熱 | 抗体検査 | － |
| | 多包虫 | 腹痛・黄疸 | 抗体検査 | ＋ |
| | 回虫 | 急な腹痛 | 虫体確認 | ＋ |
| 小腸 | ランブル鞭毛虫 | 下痢・腹痛 | 便検査(シスト，栄養体) | ＋ |
| | クリプトスポリジウム | 下痢・腹痛 | 便検査(オーシスト) | ＋ |
| | サイクロスポーラ | 下痢・腹痛 | 便検査(オーシスト) | － |
| | 横川吸虫 | 下痢・腹痛 | 便検査(虫卵) | ＋ |
| | 腸管住血吸虫(成虫) | 下痢・腹痛 | 抗体検査・便検査(虫卵) | － |
| | 広節(日本海)裂頭条虫 | 下痢・腹痛 | 虫体確認・便検査(虫卵) | ＋ |
| | 無鉤条虫 | | 虫体確認・肛門周囲虫卵検査* | － |
| | 有鉤条虫 | | 虫体確認・肛門周囲虫卵検査* | － |
| | 小型条虫 | 下痢・腹痛 | 便検査(虫卵) | ＋ |
| | 回虫 | 下痢・腹痛 | 虫体確認 | ＋ |
| | 糞線虫 | 下痢・腹痛<br>体重減少 | 便検査(幼虫) | ＋ |
| 大腸 | 赤痢アメーバ | 粘血便・下痢・腹痛 | 便検査(シスト，栄養体) | ＋ |
| | 腸管住血吸虫(成虫)* | 下痢・腹痛 | 抗体検査・便検査(虫卵) | － |
| | 鞭虫 | 下痢・腹痛(多数寄生時) | 虫体確認・便検査(虫卵) | ＋ |
| | 蟯虫 | 下痢・腹痛(多数寄生時) | 虫体確認・肛門周囲虫卵検査* | ＋ |

顎口虫と旋尾線虫タイプXはこの表に入っていない．
*いわゆるセロファンテープ法．

部症状の原因になっていることを考える．

**2.　肝異常陰影**

肝臓に寄生したり病変を引き起こす寄生虫は多い(表1)．肝臓は腫大し，慢性の季肋部痛，悪心，嘔吐，発熱などを伴う．肝臓の画像検査により何らかの異常陰影が得られるので，問題は原因の鑑別リストに寄生虫が入っているかいないかにかかっている．一般的に，寄生虫疾患の場合は，画像が派手な割に全身状態は良好である．

詳しくは「肝障害，肝脾腫，肝エコー異常」の項目で述べられるが，画像自体から寄生虫を疑う場合として「境界明瞭な肝膿瘍」がある．孤発性であればアメーバ性肝膿瘍を疑うべきだし，多発性であれば単包虫症の可能性もある．内臓幼虫移行症，肝蛭症，住血吸虫症，多包虫症などでは，肝異常陰影に加えて末梢血好酸球増多がみられる．

**3.　慢性の下痢・腹痛**

下痢が慢性的に続き，培養で起因菌が検出されず，または抗菌薬による治療が無効のときには，まず寄生虫感染を疑うべきである．通常の感染性胃腸炎は，免疫不全でなければ早くて2～3日，遅くとも1週間くらいから治癒に向かう．抗菌薬